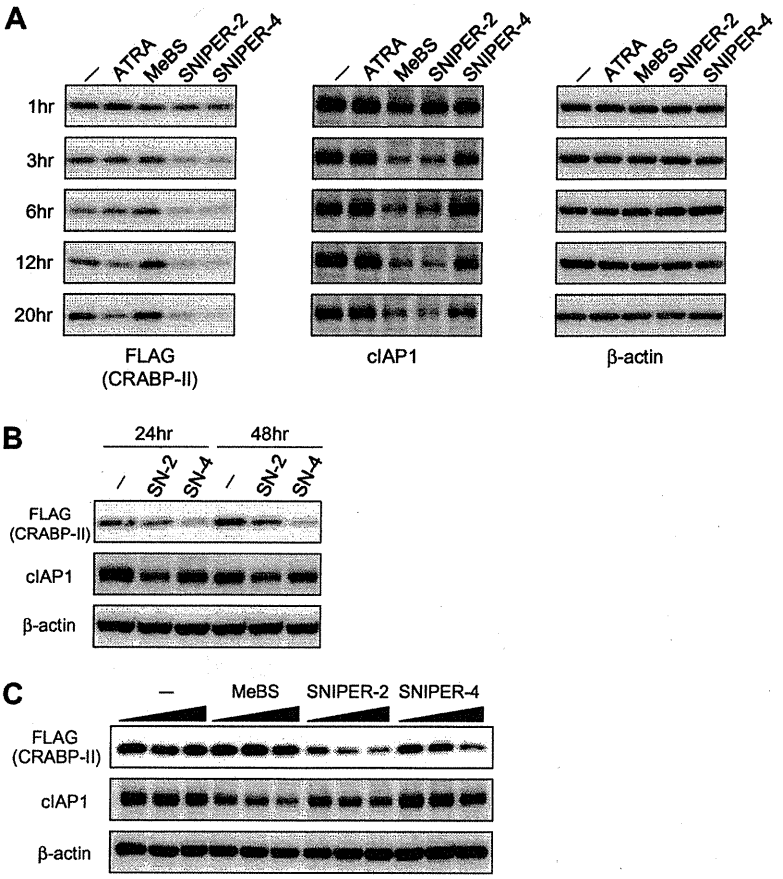

Fig. 2. (A and B) Time-course and (C) dose-dependent response of CRABP-II degradation induced by SNIPERs. HT1080 cells constitutively expressing FLAG-CRABP-II were incubated with 10 μM compounds for indicated times (A and B), or 0.3, 1 or 3 μM of compounds for 6 h (C, from the left of black triangle). Cell lysates were Western blotted with indicated antibodies.

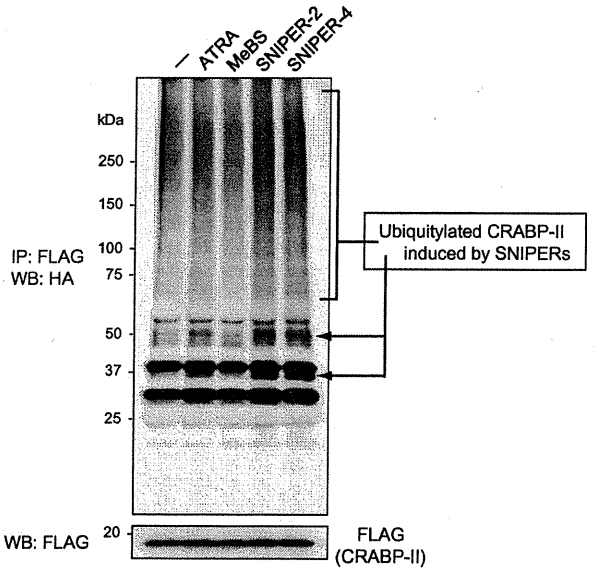

Fig. 3. Ubiquitylation of CRABP-II induced by SNIPERs. HT1080 cells expressing FLAG-CRABP-II and HA-ubiquitin were pre-treated with MG132 for 30 min, and then incubated with 10 μM of compounds for 1 h. Cells were lysed and FLAG-CRABP-II was immunoprecipitated with anti-FLAG antibody. The ubiquitylated CRABP-II was detected with anti-HA antibody.

lysis buffer (1% SDS, 0.1 M Tris–HCl (pH 7.0), 10% glycerol) and boiled for 10 min. Protein concentration was measured by BCA method (Pierce) and the equal amount of protein lysate was separated by SDS–PAGE, transferred to Hybond-P (GE Healthcare) membrane and Western blotted using appropriate antibody. Protein signals were detected using SuperSignal® West Femto Maximum Sensitivity Substrate (Thermo scientific) or ECL™ Western Blotting Detection Reagents (GE Healthcare).

2.3. Ubiquitylation of CRABP-II

HA–ubiquitin was transiently transfected in HT1080 cells constitutively expressing FLAG-CRABP-II. Cells were lysed in lysis buffer and boiled, and the lysates were diluted 10 times with 0.1 M Tris–HCl. CRABP-II was immunoprecipitated with anti-FLAG agarose-conjugated beads. The immunoprecipitates were extensively washed with diluted lysis buffer, and analyzed by Western blotting using anti-HA antibody.

3. Results and discussion

The structures of MeBS (top), SNIPER-2 (middle) and SNIPER-4 (bottom) are shown in Fig. 1A. These SNIPERs are hybrid molecules consisting of bestatin moiety and ATRA connected by an ester-bond (SNIPER-2) or an amide-bond (SNIPER-4) spacer. SNIPER-2 induces the degradation of endogenous CRABP-II and

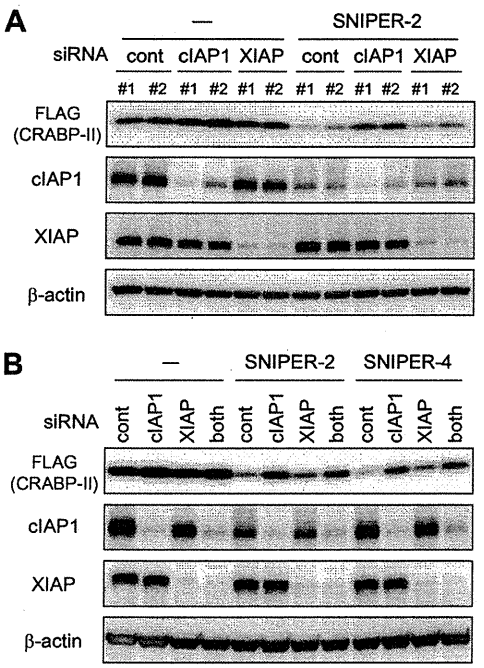

Fig. 4. Silencing of cIAP1 attenuates the SNIPER-dependent CRABP-II protein degradation. In HT1080 cells expressing FLAG-CRABP-II, the endogenous cIAP1 and XIAP were knocked down by two different siRNAs (#1 or #2) against each protein for 48 h (A). cIAP1, XIAP or both were knocked down by siRNAs (cIAP1-#1, XIAP-#2) (B). Cells were incubated with 10 μM compounds for 6 h. Shown are immunoblots of cell lysates stained with indicated antibodies.

cIAP1 in human primary fibroblasts as we reported previously (Fig. 1B) [17]. To develop a novel SNIPER that reduces CRABP-II but not cIAP1, we designed SNIPER-4 in which the ester-bond is substituted to amide-bond, because our previous study indicated that bestatin methyl amide could bind to cIAP1 without reducing it [13]. Fig. 1C shows that the SNIPER-4 reduced the level of CRABP-II but not cIAP1 in HT1080 cells as we speculated. SNIPER-2 reduced both the CRABP-II and cIAP1, while MeBS reduced cIAP1 specifically. Likewise, in HT1080 cells expressing FLAG-tagged CRABP-II, SNIPER-4 reduced FLAG-CRABP-II but not cIAP1. The combined use of MeBS and ATRA did not induce the degradation of CRABP-II (Supplementary Fig. 1). In addition, the reduction of CRABP-II by SNIPER-4 and SNIPER-2, and that of cIAP1 by MeBS and SNIPER-2, were all abrogated by a proteasome inhibitor, MG132 (Fig. 1D). These results indicate that SNIPER-2 induces proteasomal degradation of CRABP-II and cIAP1 while SNIPER-4 degrades CRABP-II specifically, and that the linking MeBS and ATRA in one molecule is required for the CRABP-II degradation.

Then, we evaluated the effect of SNIPERs on the target protein degradation, examining the reaction time-course and the treatment dose. As shown in Fig. 2A, SNIPER-2 and -4 reduce the CRABP-II at 1 h, then kept suppressing the CRABP-II expression over 20 h. On a longer time scale, the expression levels of CRABP-II at 24 or 48 h were lower in the cells treated with SNIPER-4 than with SNIPER-2 (Fig. 2B). This may be due to the maintenance of cIAP1 level in the SNIPER-4-treated cells (Fig. 2A and B), and/or the chemical stability of SNIPER-4 compared with SNIPER-2 since ester-bond is more easily hydrolyzed than amide-bond. We also tested the dose–response of SNIPERs on CRABP-II degradation. The CRABP-II was effectively reduced by over 3 μM and subtly affected by 0.3 μM or 1 μM of SNIPER-4 (Fig. 2C and Supplementary Fig. 2).

Next, we examined whether the SNIPERs induce the ubiquitylation of CRABP-II as we assumed. Lysates from the cells expressing FLAG-tagged CRABP-II and HA-tagged ubiquitin were immunoprecipitated with anti-FLAG (CRABP-II) and the immunoprecipitates were analyzed by Western blot with anti-HA (ubiquitin) to detect the ubiquitylated CRABP-II. Smear protein bands that migrate slowly in the gels increased by SNIPER-2 and SNIPER-4 (Fig. 3), which indicates the poly-ubiquitylation of CRABP-II. We further examined whether cIAP1 is the ubiquitin ligase responsible for the degradation of CRABP-II in the SNIPER-treated cells. Silencing cIAP1 expression by siRNAs significantly suppressed the SNIPER-mediated CRBAP-II degradation, whereas silencing XIAP, a close family member of cIAP1, did not (Fig. 4A and B). Expression of cIAP2, another close family member, is hardly detected in HT1080 cells (data not shown). These results indicate that cIAP1 is the primary ubiquitin ligase for CRABP-II.

Fig. 5 shows the schema of the protein knockdown by MeBS, SNIPER-2 and SNIPER-4. MeBS interacts with BIR3 domain of cIAP1 to induce auto-ubiquitylation mediated by its RING domain for proteasomal degradation (Fig. 5, top). SNIPER-2 with ester-bond cross-links cIAP1 and CRABP-II, and induces ubiquitylation of both proteins, resulting in the degradation of cIAP1 and CRABP-II by proteasome (Fig. 5, middle). SNIPER-4 with amide-bond also cross-links cIAP1 and CRABP-II, but it specifically induces proteasomal degradation of CRABP-II but not cIAP1 (Fig. 5, bottom). Thus, the amide-type SNIPER-4 would be more useful than the ester-type SNIPER-2 for protein knockdown in terms of the specificity and prolonging the duration of the degradation process.

The reason why SNIPER-4 does not degrade cIAP1 is not fully understood. We previously reported that bestatin-methyl ester (MeBS) induced proteasomal degradation of cIAP1, whereas bestatin-methyl amide (BE-04) did not (13). Therefore, we hypothesize that BE-04 and SNIPER-4 with amide-bond would not induce auto-ubiquitylation of cIAP1, or if any it is not enough for efficient proteasomal degradation. Probably, the robustness and/or kinetics of the auto-ubiquitylation would be much lower than that induced by MeBS and SNIPER-2 with ester-bond, and therefore, de-ubiquitylation of cIAP1 quickly occurs to prevent degradation.

To study physiological functions of certain proteins, genetic knockdown by RNA interference or genetic knockout by gene targeting was commonly applied for suppressing the expression. Comparing with such genetic methods, the protein knockdown by SNIPERs has several advantages: (i) SNIPERs are small molecules and easily delivered into cells, which is especially advantageous for medical application in future. (ii) The degradation of the target protein begins soon after the addition of SNIPERs, and therefore the protein knockdown is attained in several hours. We suppose that the protein knockdown by SNIPERs could be a complementary technology to RNA interference, and if combined it may be possible to downregulate a target protein more rapidly and robustly. This is especially the case for a long-lived protein that is insufficiently downregulated by RNA interference alone.

The protein knockdown by SNIPERs depends on cIAP1-mediated ubiquitylation of the target protein. The cIAP1 is ubiquitously expressed in a variety of tissues and cells [18], indicating that the protein knockdown by SNIPERs would be attained in most tissues and cells expressing cIAP1. Since cIAP1 is involved in NFκB signaling in some cells, the effect of SNIPERs on normal cell function should be carefully investigated. Structurally, SNIPERs could target other proteins for degradation if ATRA is substituted to ligands for other target proteins. We propose the amide-type SNIPER could be applicable to downregulate pathogenic proteins for therapeutic purposes.

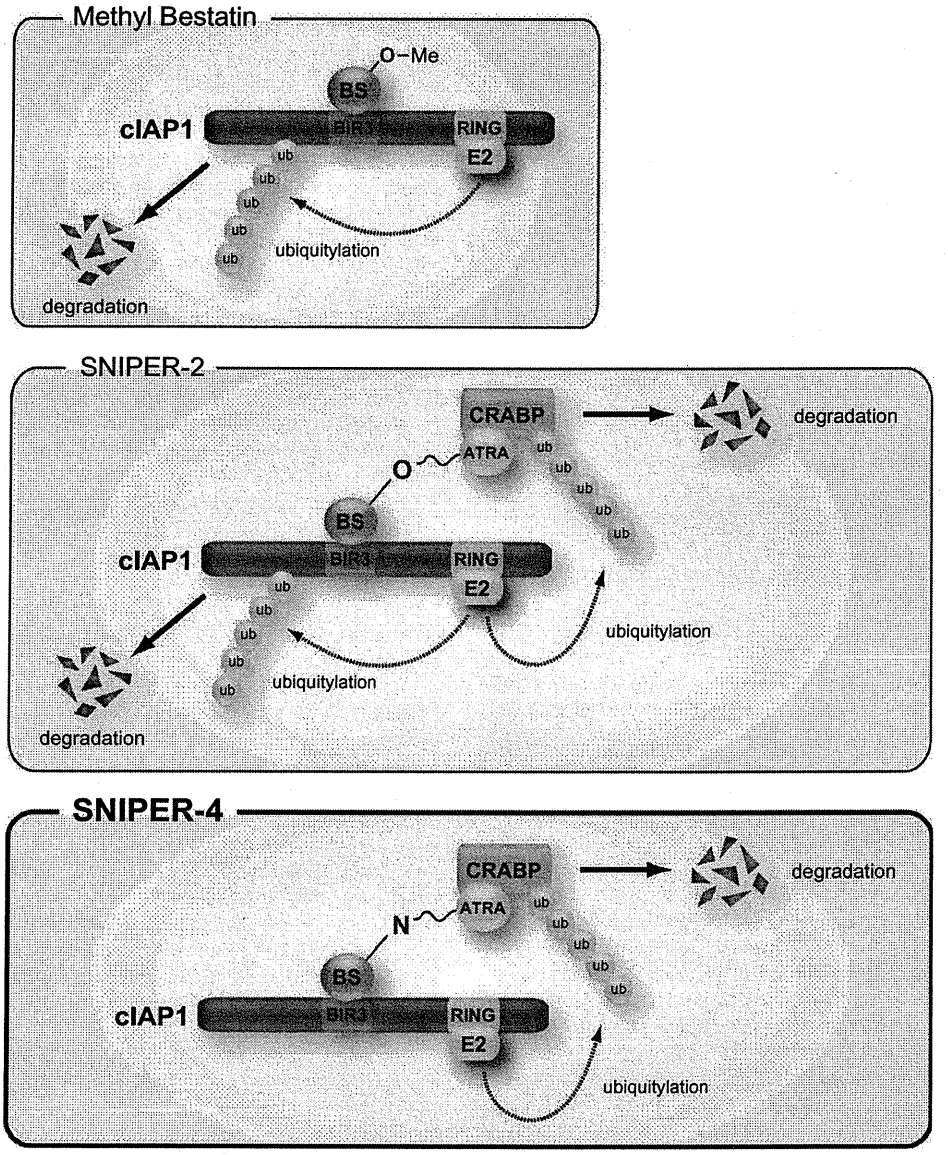

Fig. 5. Scheme of the protein knockdown by MeBS (top), SNIPER-2 (middle) and SNIPER-4 (bottom). See text for the explanation.

Acknowledgements

We thank Nippon Kayaku Co. Ltd., for kindly providing MeBS. This study was supported in part by Grants-in-Aids for Cancer Research from the Ministry of Education, Culture, Sports, Science and Technology, Japan, and by the research grant of Astellas Foundation for Research on Metabolic Disorders.

Appendix A. Supplementary data

Supplementary data associated with this article can be found, in the online version, at doi:10.1016/j.febslet.2011.03.019.

References

[1] Glickman, M.H. and Ciechanover, A. (2002) The ubiquitin–proteasome proteolytic pathway: destruction for the sake of construction. Physiol. Rev. 82, 373–428.
[2] Bader, M. and Steller, H. (2009) Regulation of cell death by the ubiquitin–proteasome system. Curr. Opin. Cell Biol. 21, 878–884.
[3] Nakayama, K.I. and Nakayama, K. (2006) Ubiquitin ligases: cell-cycle control and cancer. Nat. Rev. Cancer 6, 369–381.
[4] Jiang, Y.H. and Beaudet, A.L. (2004) Human disorders of ubiquitination and proteasomal degradation. Curr. Opin. Pediatr. 16, 419–426.
[5] Zhou, X., Wang, J.L., Lu, J., Song, Y., Kwak, K.S., Jiao, Q., Rosenfeld, R., Chen, Q., Boone, T., Simonet, W.S., Lacey, D.L., Goldberg, A.L. and Han, H.Q. (2010) Reversal of cancer cachexia and muscle wasting by ActRIIB antagonism leads to prolonged survival. Cell 142, 531–543.
[6] Morris, L.G., Veeriah, S. and Chan, T.A. (2010) Genetic determinants at the interface of cancer and neurodegenerative disease. Oncogene 29, 3453–3464.
[7] Hoeller, D., Hecker, C.M. and Dikic, I. (2006) Ubiquitin and ubiquitin-like proteins in cancer pathogenesis. Nat. Rev. Cancer 6, 776–788.
[8] Ito, T., Ando, H., Suzuki, T., Ogura, T., Hotta, K., Imamura, Y., Yamaguchi, Y. and Handa, H. (2010) Identification of a primary target of thalidomide teratogenicity. Science 327, 1345–1350.
[9] Sakamoto, K.M., Kim, K.B., Kumagai, A., Mercurio, F., Crews, C.M. and Deshaies, R.J. (2001) Protacs: chimeric molecules that target proteins to the Skp1-Cullin-F box complex for ubiquitination and degradation. Proc. Natl. Acad. Sci. USA 98, 8554–8559.
[10] Srinivasula, S.M. and Ashwell, J.D. (2008) IAPs: what's in a name? Mol. Cell 30, 123–135.

[11] Vaux, D.L. and Silke, J. (2005) IAPs, RINGs and ubiquitylation. Nat. Rev. Mol. Cell Biol. 6, 287–297.
[12] Gyrd-Hansen, M. and Meier, P. (2010) IAPs: from caspase inhibitors to modulators of NF-kappaB, inflammation and cancer. Nat. Rev. Cancer 10, 561–574.
[13] Sekine, K., Takubo, K., Kikuchi, R., Nishimoto, M., Kitagawa, M., Abe, F., Nishikawa, K., Tsuruo, T. and Naito, M. (2008) Small molecules destabilize cIAP1 by activating auto-ubiquitylation. J. Biol. Chem. 283, 8961–8968.
[14] Kim, S., Ohoka, N., Okuhira, K., Sai, K., Nishimaki-Mogami, T. and Naito, M. (2010) Modulation of RIP1 ubiquitylation and distribution by MeBS to sensitize cancer cells to tumor necrosis factor alpha-induced apoptosis. Cancer Sci. 101, 2425–2429.
[15] Sato, S., Aoyama, H., Miyachi, H., Naito, M. and Hashimoto, Y. (2008) Demonstration of direct binding of cIAP1 degradation-promoting bestatin analogs to BIR3 domain: synthesis and application of fluorescent bestatin ester analogs. Bioorg. Med. Chem. Lett. 18, 3354–3358.
[16] Sato, S., Tetsuhashi, M., Sekine, K., Miyachi, H., Naito, M., Hashimoto, Y. and Aoyama, H. (2008) Degradation-promoters of cellular inhibitor of apoptosis protein 1 based on bestatin and actinonin. Bioorg. Med. Chem. 16, 4685–4698.
[17] Itoh, Y., Ishikawa, M., Naito, M. and Hashimoto, Y. (2010) Protein knockdown using methyl bestatin-ligand hybrid molecules: design and synthesis of inducers of ubiquitination-mediated degradation of cellular retinoic acid-binding proteins. J. Am. Chem. Soc. 132, 5820–5826.
[18] Uren, A.G., Pakusch, M., Hawkins, C.J., Puls, K.L. and Vaux, D.L. (1996) Cloning and expression of apoptosis inhibitory protein homologs that function to inhibit apoptosis and/or bind tumor necrosis factor receptor-associated factors. Proc. Natl. Acad. Sci. USA 93, 4974–4978.

Bioorganic & Medicinal Chemistry 19 (2011) 3229–3241

Contents lists available at ScienceDirect

Bioorganic & Medicinal Chemistry

journal homepage: www.elsevier.com/locate/bmc

Development of target protein-selective degradation inducer for protein knockdown

Yukihiro Itoh [a], Minoru Ishikawa [a], Risa Kitaguchi [a], Shinichi Sato [a], Mikihiko Naito [b], Yuichi Hashimoto [a,*]

[a] Institute of Molecular and Cellular Biosciences, The University of Tokyo, 1-1-1 Yayoi, Bunkyo-ku, Tokyo 113-0032, Japan
[b] National Institute of Health Sciences, 1-18-1 Kamiyoga, Setagaya-ku, Tokyo 158-8501, Japan

ARTICLE INFO

Article history:
Received 10 March 2011
Revised 22 March 2011
Accepted 24 March 2011
Available online 29 March 2011

Keywords:
Protein knockdown
Protein degradation inducer
IAPs
CRABP-II

ABSTRACT

Our previous technique for inducing selective degradation of target proteins with ester-type SNIPER (Specific and Nongenetic Inhibitor-of-apoptosis-proteins (IAPs)-dependent Protein ERaser) degrades both the target proteins and IAPs. Here, we designed a small-molecular amide-type SNIPER to overcome this issue. As proof of concept, we synthesized and biologically evaluated an amide-type SNIPER which induces selective degradation of cellular retinoic acid binding protein II (CRABP-II), but not IAPs. Such small-molecular, amide-type SNIPERs that induce target protein-selective degradation without affecting IAPs should be effective tools to study the biological roles of target proteins in living cells.

1. Introduction

Methods to down-regulate target proteins in cells or animals are useful not only for biological studies and medical research, but also for developing therapeutic strategies in cases where expression of a target protein is involved in the pathogenesis of disease. Thus far, deletion and suppression of proteins at the pre-translational level by means of gene knockout and gene knockdown have been widely used for ablating target proteins. Such techniques have yielded insight into the biological functions of numerous proteins in cells or animals. However, complicated and time-consuming genetic manipulation is required for gene knockout. Gene knockdown using RNA interference is easy, but cannot remove existing proteins and so is especially ineffective for proteins with a long half-life. Therefore, the utility of these genetic methods for medical applications is limited. Proteolysis-targeting chimeric molecules (protacs) represent a pioneering approach in the field of down-regulating proteins post-translationally.[1] However, the membrane permeability or stability of peptide structures is often inadequate for biological studies and therapeutic applications.[2] Therefore, new general techniques, which overcome these issues, are needed.

Recently, we have reported protein knockdown as a technique for inducing selective degradation of proteins post-translationally by using small molecules which have sufficient membrane permeability.[3] This approach mimics physiological caspase degradation by inhibitor of apoptosis proteins (IAPs), which show ubiquitin ligase (E3) activity.[4,5] Under physiological conditions, caspase degradation occurs via two steps: (i) IAPs bind to caspases and promote poly-ubiquitination, (ii) the polyubiquitinated caspases are degraded by proteasome (Fig. 1a). Protein knockdown is achieved by the use of small molecules designed as conjugates of an IAP recognition moiety with a specific ligand for a target protein. Such a molecule, which we named SNIPER (Specific and Nongenetic IAPs-dependent Protein ERaser), induces formation of an artificial (non-physiological) complex of IAP and the target protein, thereby promoting poly-ubiquitination and proteasomal degradation of the target protein (Fig. 1b). We adopted methyl bestatin (MeBS, **2**) (Fig. 1)[6,7] as a ligand for cellular inhibitor of apoptosis protein 1 (cIAP1), which is one of the IAPs,[5,8] and all-*trans* retinoic acid (ATRA, **3**) (Fig. 2) as a specific ligand for cellular retinoic acid binding protein II (CRABP-II),[9] and synthesized SNIPER (**4**) (Fig. 3)[3] as a tool for degradation of CRABP-II. However, this ester-type SNIPER (**4**) was found to promote auto-degradation of cIAP1, like MeBS (**2**),[3,6,7] and thus, the selectivity of ester-type SNIPER (**4**) for its target protein is poor. In addition, the ester group of **4** might be easily hydrolyzed in cells. Therefore, we aimed to develop a new type of SNIPER which would overcome these problems. Herein, we describe the design, synthesis and biological evaluation of an amide-type SNIPER which induces selective degradation of CRABP-II, without affecting IAPs.

2. Chemistry

The compounds prepared for this study are shown in Figure 3 (compounds **5–8**) and Figure 6 (DanBE, **16**). Syntheses were carried

* Corresponding author. Tel.: +81 3 5841 7847; fax: +81 3 5841 8495.
E-mail address: hashimot@iam.u-tokyo.ac.jp (Y. Hashimoto).

0968-0896/$ - see front matter © 2011 Elsevier Ltd. All rights reserved.
doi:10.1016/j.bmc.2011.03.057

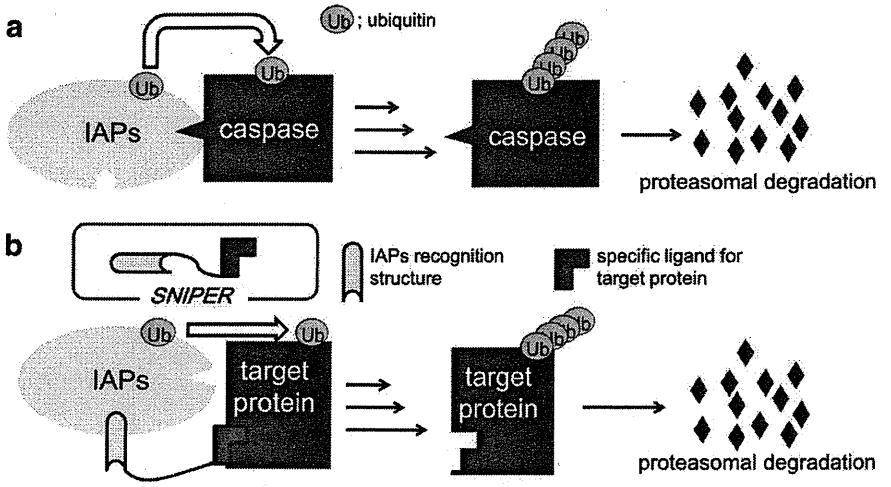

Figure 1. (a) Physiological protein degradation. (b) Artificial protein degradation (protein knockdown) induced by SNIPER.

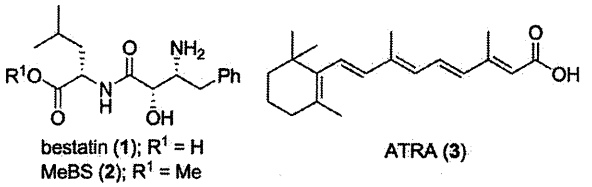

Figure 2. Structures of bestatin (**1**), bestatin methyl ester (MeBS, **2**), and ATRA (**3**).

out as outlined in Schemes 1–3. The route for synthesis of compounds **5** and **7** is illustrated in Scheme 1. Condensation of amine **10** with acid **11** afforded amide **12**. Hydrolysis of ester **12** under an alkaline condition gave acid **14**. Bestatin (**1**) was treated with di-*tert*-butyl dicarbonate ($(Boc)_2O$) to yield *N*-Boc bestatin (**13**). Condensation of acid **13** or **14** with methylamine afforded amides **15** and **7**. Removal of the Boc group of **15** gave BE04 (**5**).

DanBE (**16**) was synthesized from **17** and **18** via the route shown in Scheme 2. Condensation of sulfonyl chloride **17** with amine **18** gave sulfonamide **19**. Alcohol **19** was allowed to react with *N*-Boc bestatin (**14**) and subsequent deprotection of the Boc group of compound **20** gave DanBE (**16**).

Compounds **6** and **8** were synthesized as outlined in Scheme 3. Alcohol **21**[10] was converted to azide **23** by tosylation and subsequent treatment with sodium azide. Amine **24**, obtained by reduction of azide **23**, was allowed to react with compounds **14** and **25**[3] to yield amides **26** and **27**. Condensation of acid **28**[3] with amines **29** and **30**, derived by deprotection of the Boc group of compounds **26** and **27**, afforded amides **31** and **32**. Deprotection of the 2-cyanoethyl groups of compounds **31** and **32** with tetrabutylammonium fluoride (TBAF) gave acid **33** and compound **8**.[3,11] Removal of the 9-fluorenylmethyloxycarbonyl (Fmoc) group of compound **33** with 1,8-diazabicyclo[5.4.0]undec-7-ene (DBU)[3,12] gave compound **6**.

3. Results and discussion

3.1. Molecular design

We selected MeBS (**2**) as a ligand for cIAP1 in the previous study because MeBS (**2**) activates auto-ubiquitination of cIAP1 and

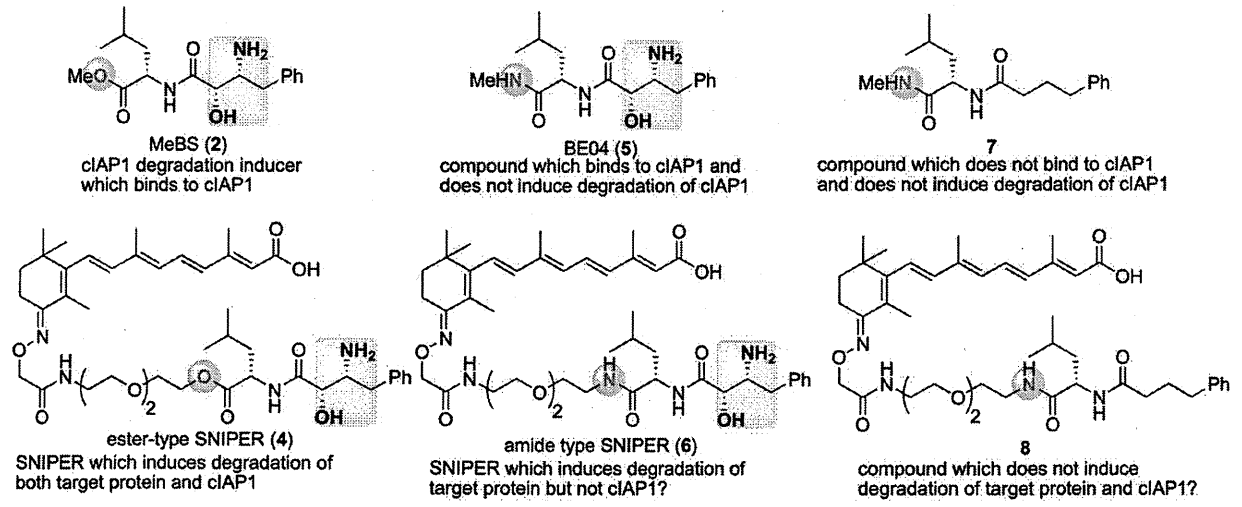

Figure 3. Structures and molecular design of SNIPERs.

maintains the E3 activity of cIAP1. Therefore, we considered that highly selective SNIPERs might be obtained by replacement of MeBS (**2**) in the ester-type SNIPER (**4**) with a structure which binds to cIAP1, but does not induce auto-degradation of cIAP1 and does not inhibit the E3 activity of cIAP1. Therefore we attempted to identify such a structure. Naito's group investigated the cIAP1-binding affinity and auto-degradation activity of MeBS analogs.[6] The order of binding affinity evaluated by means of surface plasmon resonance (SPR) binding experiments indicated that the binding affinity of BE04 (**5**) (Fig. 3) is higher than that of bestatin (**1**), which induced degradation of cIAP1, but lower than that of MeBS (**2**). On the other hand, the cIAP1-degradation activity of BE04 (**5**) is apparently weaker than that of bestatin (**1**) or MeBS (**2**).[6] These results indicate that the two activities (binding activity and auto-degradation activity) should be separable. We further investigated the effect of BE04 (**5**) on cIAP1 levels by means of Western blotting. Treatment of HT1080 cells expressing FLAG-tagged cIAP1 with even 1000 μM BE04 (**5**) had no influence on cIAP1 levels (Fig. 4a–c). Accordingly, it appears that BE04 (**5**) does not induce auto-degradation of cIAP1. In addition, the results shown in Figure 5 indicate that BE04 (**5**) has no influence on E3 activity, because ubiquitination of cIAP1 is mainly mediated by the E3 activity of cIAP1 itself.[13] Next, we investigated the binding of BE04 (**5**) to cIAP1. The results of fluorescence polarization (FP) assay[7] indicated that BE04 (**5**) did bind to cIAP1 (Fig. 6) and showed competitive binding with respect to DanBE (**16**),[7] a FP probe. Moreover, it was suggested that BE04 (**5**) and MeBS (**2**) bound to cIAP1 in a mutually competitive manner by means of Western blot analysis (Fig. 4b). Taken together, these results indicate that BE04 (**5**) has the activity we expected. Therefore, it appears that substitution of the ester group of **4** to amide greatly decreases cIAP1-degradation activity, but the binding affinity is partially retained and the amide has no influence on E3 activity. This substitution is also expected to be advantageous for prolonging the duration of target protein destabilization, because amide groups are generally more stable than ester groups in the intracellular environment. Based on these findings, we designed and synthesized SNIPER (**6**) as a selective degradation inducer of CRABP (Fig. 3). We also prepared compound **8** as a negative control (Fig. 3), based on compound **7**,[14] which does not bind to cIAP1 and does not induce auto-degradation of cIAP1 (Figs. 4a, c and 6).

3.2. Selectivity and time course of degradation of CRABP-II by the synthesized compound

We initially evaluated the cIAP1/CRABP-II degradation selectivity of SNIPER (**6**) and compound **8**. The CRABP-II degradation activity of **6** was similar to that of SNIPER (**4**) as evaluated by Western blot analysis. As expected, **6** had no influence on cIAP1 levels even at 30 μM (Fig. 7a and b). On the other hand, compound **8** did not induce degradation of either cIAP1 or CRABP-II (Fig. 7a). Next we examined whether **6** induced degradation of X-linked inhibitor of apoptosis protein (XIAP) and cellular inhibitor of apoptosis protein 2 (cIAP2), which (i) are members of the IAP family, (ii) have E3 activity, and (iii) induce auto-degradation.[5,8] As shown in Figs. 4b, c, and 6 had no effect on the levels of XIAP and cIAP2, as was the case for BE04 (**5**) (Fig. 7c and d). These results indicated that amide-type SNIPER (**6**) had high specificity for degradation of CRABP-II. In addition, the reduced CRABP-II level was maintained for 12 h with **4**, whereas it was maintained for 48 h with **6** (Fig. 7e). The replacement of the ester group with amide thus greatly prolonged the duration of CRABP-II destabilization.

We next confirmed the mechanism of CRABP-II degradation by **6**, using the previously reported methods,[3] including pretreatment

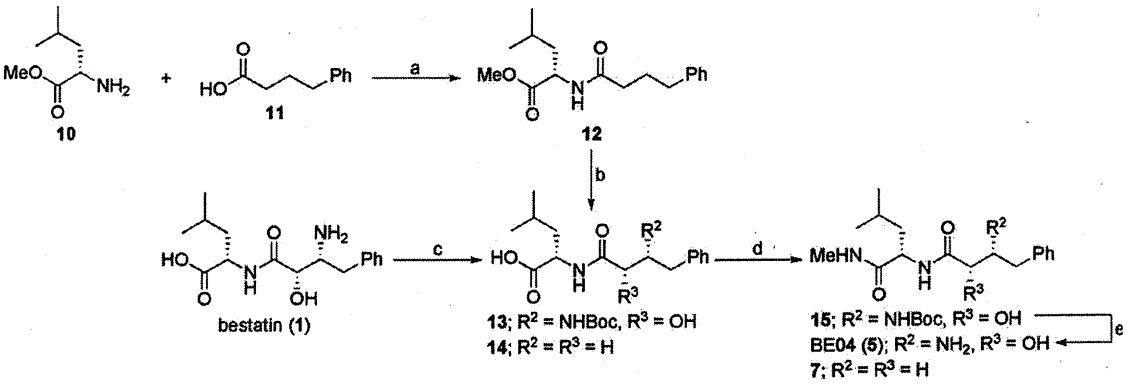

Scheme 1. Reagents and conditions: (a) 1-ethyl-3-(3-dimethylaminopropyl)carbodiimide hydrochloride (EDCI), 1-hydroxybenzotriazole hydrate (HOBt·H_2O), Et_3N, tetrahydrofuran (THF), rt, 100%; (b) LiOH, MeOH, H_2O, rt, 93%; (c) di-*tert*-butyl dicarbonate, NaOH, H_2O, acetone, rt, 61%; (d) methylamine hydrochloride, EDCI, HOBt·H_2O, iPr_2NEt, dimethylformamide (DMF), CH_2Cl_2, rt, 88–99%; (e) HCl, 1,4-dioxane, rt, 99%.

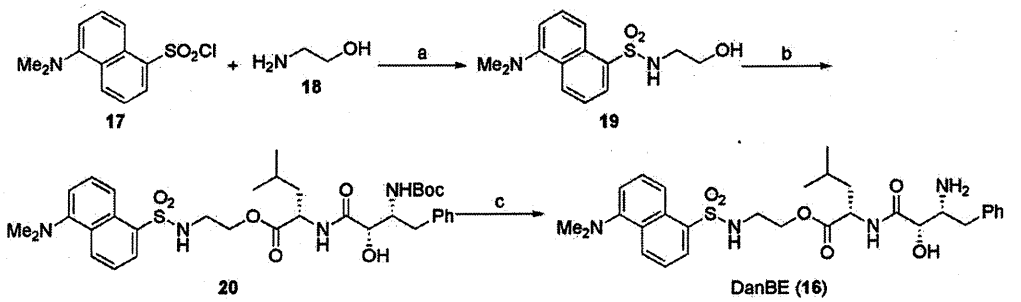

Scheme 2. Reagents and conditions: (a) Et_3N, CH_2Cl_2, rt, 68%; (b) *N*-Boc bestatin (**13**), EDCI, HOBt·H_2O, iPr_2NEt, CH_2Cl_2, rt, 24%; (c) HCl, 1,4-dioxane, CH_2Cl_2, rt, 100%.

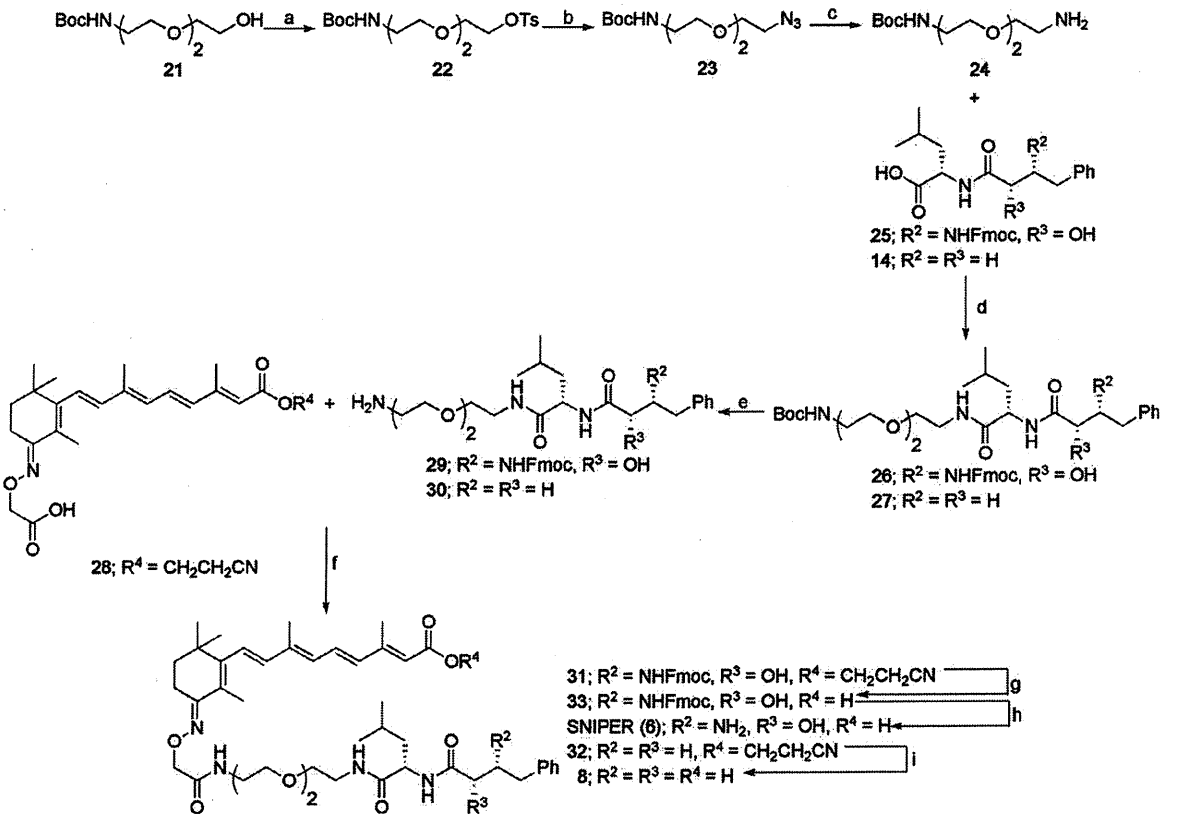

Scheme 3. Reagents and conditions: (a) *p*-toluenesulfonyl chloride, *N*,*N*-dimethylaminopyridine (DMAP), Et_3N, CH_2Cl_2, rt; (b) NaN_3, DMF, 60 °C, 98% (two steps); (c) Pd/C, H_2, EtOH, rt, quant.; (d) EDCI, HOBt·H_2O, CH_2Cl_2, rt, 78–88%; (e) HCl, 1,4-dioxane, CH_2Cl_2, quant.; (f) EDCI, HOBt·H_2O, THF, rt, 56–62%; (g) tetrabutylammonium fluoride (TBAF), MeOH, THF, rt; (h) 1,8-diazabicyclo[5.4.0]undec-7-ene (DBU), *n*-$C_{12}H_{25}SH$, CH_2Cl_2, rt, 57% (two steps); (i) TBAF, MeOH, THF, rt, 70%.

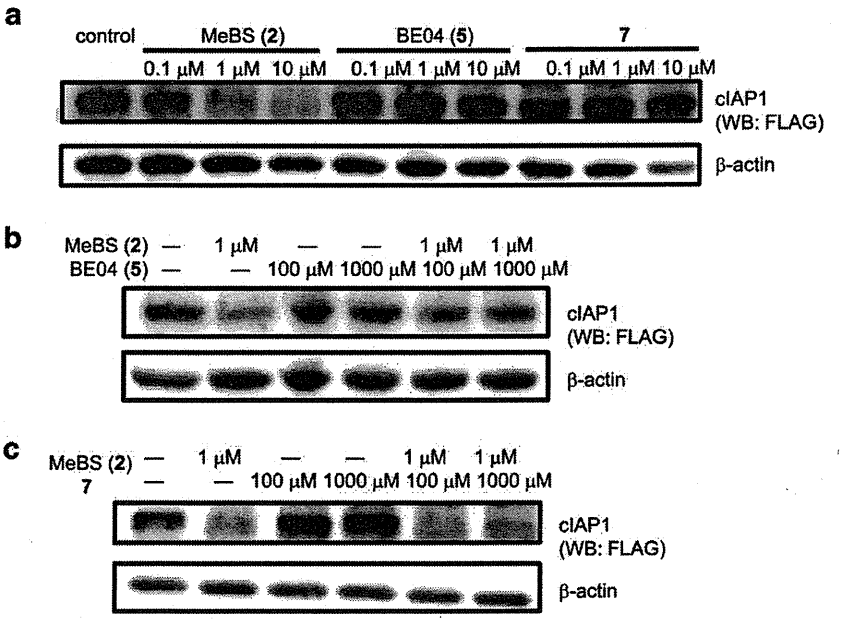

Figure 4. (a) Western blot-detection of cIAP1 levels in HT1080 cells expressing FLAG-tagged cIAP1. The cells were treated with compounds for 6 h. (b) BE04 (**5**) or (c) compound **7** was added to the culture 1 h prior to the addition of MeBS (**2**). BE04 (**5**) inhibited degradation of cIAP1 by MeBS (**2**) and compound **7** did not. These results suggested that: (i) BE04 (**5**) and compound **7** do not induce degradation of cIAP1, (ii) BE04 (**5**) and MeBS (**2**) bind to cIAP1 in a mutually competitive manner in cells, but compound **7** and MeBS (**2**) do not show competitive binding.

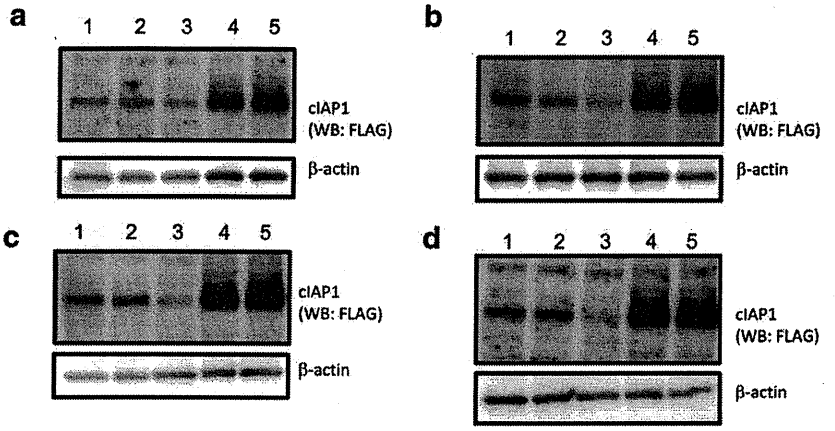

Figure 5. Western blot-detection of cIAP1 levels in HT1080 cells expressing FLAG-tagged cIAP1 after (a) 15-min, (b) 30-min, (c) 60-min, and (d) 120-min treatment with reagents. MG132 was added to the culture 30 min prior to the addition of MeBS (**2**) or BE04 (**26**). Lane 1, control; lane 2, 1000 μM BE04 (**26**); lane 3, 30 μM MeBS (**2**); lane 4, 10 μM MG132; lane 5, mixture of 10 μM MG132 and 1000 μM BE04 (**26**). Proteasome inhibitor MG132 inhibited auto-degradation of cIAP1 and increased the accumulation of cIAP1, but BE04 (**5**) had no influence on cIAP1 level. In addition, BE04 (**5**) had no influence on the accumulation of cIAP1 induced by MG132 (lanes 4 and 5). Given that ubiquitination and degradation of cIAP1 are mediated by the ubiquitin ligase activity of cIAP1 itself,[8] these results indicate that BE04 (**5**) did not inhibit the ubiquitin ligase activity of cIAP1.

with an excess of MeBS (**2**) (Fig. 8a), GST pull-down assay (Fig. 8b), combined use of proteasome inhibitors (Fig. 8c), combined use of MeBS (**2**) or BE04 (**5**) and ATRA (**3**) (Fig. 9), RARα degradation assay and RAR reporter gene assay (data not shown). In these mechanistic analyses, all actions of **6** were similar to those of **4**, except for degradation activity towards cIAP1. Therefore, SNIPER (**6**) is suggested to induce (i) formation of an artificial ternary complex with cIAP1 and CRABP-II, (ii) ubiquitination of CRABP-II by cIAP1, and (iii) degradation of ubiquitinated CRABP-II by proteasome.[3]

3.3. Effect on cIAP1 inhibition at the level of function by the synthesized compound

Although amide-type SNIPER (**6**) degraded CRABP-II without affecting cIAP1 levels, **6** may inhibit the biological function of cIAP1, because it binds to cIAP1. Such inhibition would be unfavorable for investigation of the biological function of a target protein by protein knockdown. Therefore, we investigated whether **6** inhibits the function of cIAP1. It is thought that inhibition of IAP function activates caspase 3/7 and induces apoptosis.[5,15] Indeed, cIAP1 destabilization by MeBS (**2**) enhanced apoptosis of cancer cells by chemotherapeutic drugs such as cisplastin and etoposide (ETP).[6] Therefore, we evaluated the effect on apoptosis in HT1080 cells of MeBS (**2**), ester-type SNIPER (**4**) and **6** in the presence or absence of ETP, using lactate dehydrogenase (LDH) assay (Fig. 10a). In the absence of etoposide, MeBS (**2**), **4**, and **6** hardly induced apoptosis. However, MeBS (**2**) and **4**, which induce cIAP1 degradation, enhanced apoptosis of HT1080 cells by ETP in a dose-dependent fashion, while **6**, which has no effect on cIAP1 levels, did not enhance apoptosis of HT1080 cells. Furthermore, we investigated the effects of these compounds on caspase 3/7 activation. As shown in Figure 10b, these compounds did not activate caspase 3/7 in the absence of ETP. In the presence of ETP, MeBS (**2**) and **4** activated caspase 3/7, whereas **6** had no effect on caspase 3/7. Collectively, these results suggest that the binding of **6** to cIAP1 neither induces degradation of cIAP1 nor inhibits cIAP1 function. All the results mentioned above indicated that amide-type SNIPER (**6**) exhibits satisfactory selectivity and stability, overcoming the issues found in the case of ester-type SNIPER.

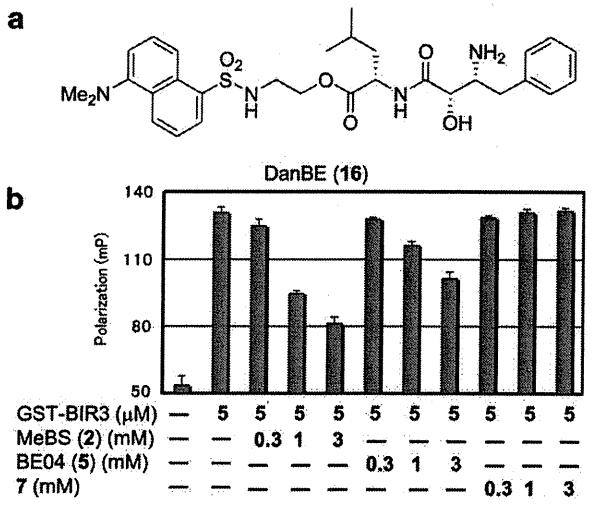

Figure 6. (a) Structure of DanBE (**16**), a fluorescence polarization (FP) probe. (b) Binding assay. Competitive displacement studies were performed with MeBS (**2**), BE04 (**5**), and compound **7** by means of FP assay. MeBS (**2**), BE04 (**5**) or compound **7** was incubated in the presence of DanBE (**16**) and GST-BIR-3 (GST-tagged BIR3 domain of cIAP1, to which MeBS (**2**) binds) for 5 min at room temperature in phosphate-buffered saline (pH 7.4). After incubation, the fluorescence polarization of DanBE (**16**) was measured.

3.4. Characterization of CRABP-II in neuroblastoma cells using SNIPER

Finally, we attempted to demonstrate that amide-type SNIPER is useful for investigation of the biological function of CRABP-II by protein knockdown. It was reported that CRABP-II increases expression of the oncogene MycN in neuroblastoma cells.[16] In addition, MycN inhibits caspase and the apoptotic pathway[17] and MycN knockdown inhibits proliferation of neuroblastoma cells.[18] Therefore, we investigated the effects of amide-type SNIPER (**6**) on MycN expression, caspase activation and proliferation of neuroblastoma cells. Consistent with the reported role of CRABP-II in MycN expression, **6** decreased MycN levels (Fig. 11a) concomitantly with a decrease of CRABP-II protein (Fig. 11b). Next, we investigated the effects of MeBS (**2**), BE04 (**5**), and **6** on caspase 3/7 in IMR-32 cells (Fig. 11c). MeBS (**2**) and BE04 (**5**) hardly activated caspase 3/7, whereas **6** significantly activated caspase

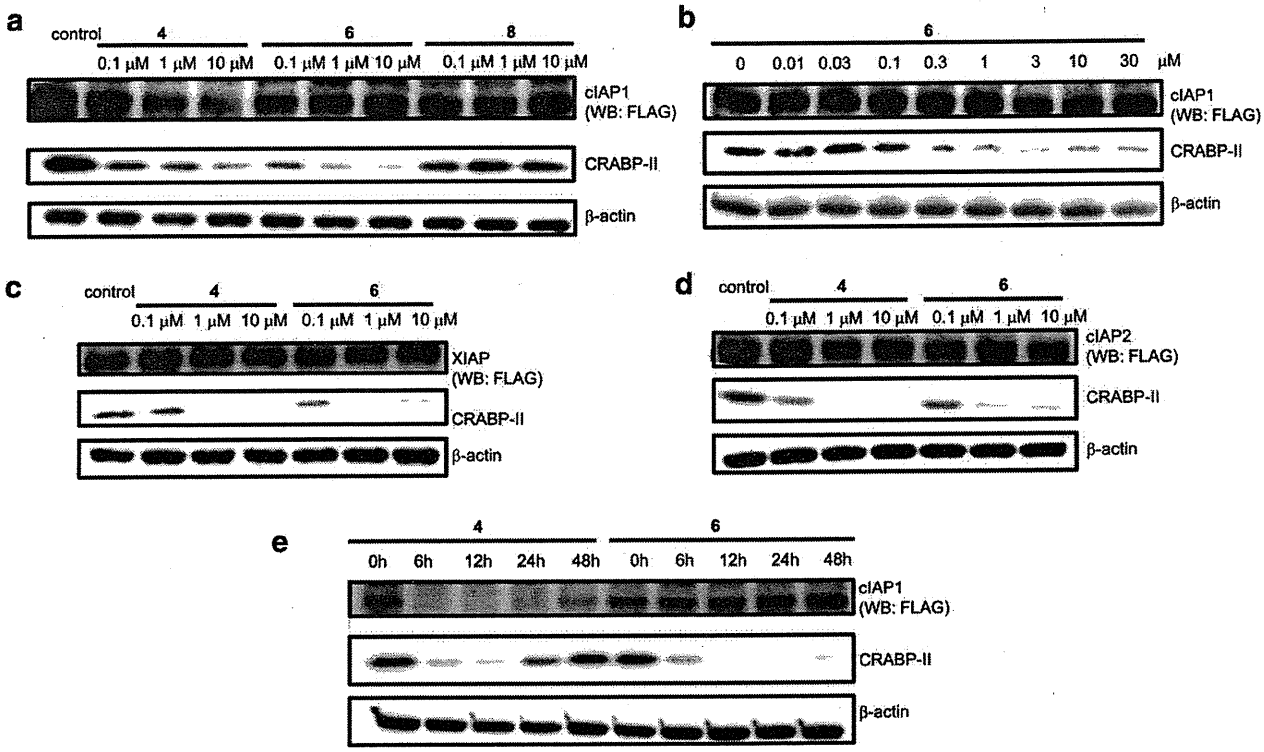

Figure 7. (a) Western blot-detection of CRABP-II levels in HT1080 cells expressing FLAG-tagged cIAP1 after 6-h treatment with compounds **4**, **6**, and **8**. (b) Western blot-detection of CRABP-II and cIAP1 levels in HT1080 cells expressing FLAG-tagged cIAP1 after 6-h treatment with SNIPER (**6**). Compound **6** induced dose-dependent down-regulation of CRABP-II, but not cIAP1. (c) Western blot-detection of XIAP levels in HT1080 cells expressing FLAG-tagged XIAP. The cells were treated with compounds for 6 h. (d) Western blot-detection of cIAP2 levels in HT1080 cells expressing FLAG-tagged cIAP2. The cells were treated with compounds for 6 h. (e) Western blot-detection of cIAP1 levels and CRABP-II in HT1080 cells expressing FLAG-tagged cIAP1 treated with ester-type SNIPER (**4**) and amide-type SNIPER (**6**). With **4**, the reduced CRABP-II level was maintained for 12 h whereas with **6**, it was maintained for 48 h.

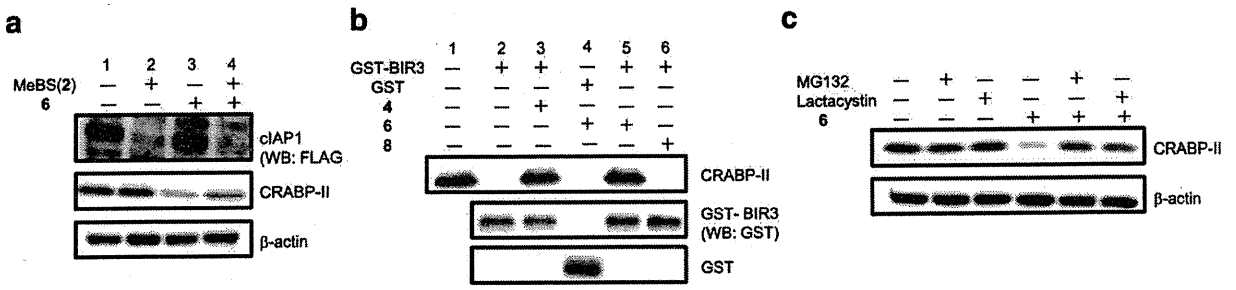

Figure 8. (a) Influence of pretreatment of HT1080 cells expressing FLAG-tagged cIAP1 with MeBS (**2**) on induction of CRABP-II degradation. The cells were treated with 1 μM **6** for 6 h. MeBS (**2**) (1000 μM) was added to the culture 1 h prior to the addition of **6**. Pretreatment with an excess amount of MeBS (**2**) led to the complete disappearance of cIAP1 (lane 2). CRABP-II levels were down-regulated by treatment with amide-type SNIPER (**6**) [without pretreatment with MeBS (**2**)] as mentioned above (lane 3), whereas amide-type SNIPER (**6**) scarcely decreased the CRABP-II levels in cells pretreated with 1000 μM MeBS (**2**) (lane 4). These results indicate that the reduction of CRABP-II by amide-type SNIPER (**6**) is mediated by cIAP1. (b) Western blot-detection of GST-BIR3, GST, and CRABP-II levels of samples prepared by pull-down assay in vitro: lane 1, CRABP-II levels; lane 2, mixture of GST-BIR3 and CRABP-II; lane 3, mixture of GST-BIR3, CRABP-II, and **4**; lane 4, mixture of GST, CRABP-II, and **6**; lane 5, mixture of GST-BIR3, CRABP-II, and **6**; lane 6, mixture of GST-BIR3, CRABP-II, and **8**. GST-BIR3 pulled down CRABP-II in the presence of amide-type SNIPER (**6**) (lane 5) as well as ester-type SNIPER (**4**) (lane 3), but not in the absence of amide-type SNIPER (**6**) (lane 2) or in the presence of compound **8** (lane 6). GST did not co-precipitate CRABP-II even in the presence of amide-type SNIPER (**6**) (lane 4). This result indicates that CRABP-II is held in proximity to cIAP1 by amide-type SNIPER (**6**), but not by compound **8**. (c) Influence of pretreatment with proteasome inhibitors on induction of CRABP-II degradation. Western blot-detection of CRABP-II level in HT1080 cells expressing FLAG-tagged cIAP1. The cells were treated with 1 μM **6** for 6 h. MG132 (10 μM) and lactacystin (10 μg/mL) were added to the culture 30 min prior to the addition of **6**. The down-regulation of CRABP-II by amide-type SNIPER (**6**) was cancelled by proteasome inhibitors, MG132 and lactacystin. This result suggested that the down-regulation of CRABP-II induced by amide-type SNIPER (**6**) is mediated by proteasomal degradation.

3/7. Finally, we evaluated inhibition of cell proliferation by MeBS (**2**), BE04 (**5**), and **6**, using IMR-32 cells (Fig. 12). The results were consistent with the results of caspase 3/7 assay. MeBS (**2**) and BE04 (**5**) did not show strong inhibition of cell proliferation, whereas **6** showed strong and dose-dependent inhibition. On the other hand, **6** hardly inhibited proliferation of HT1080 and MCF-7 cells, which express CRABP-II and cIAP1, but not MycN, though it decreased CRABP-II in these cells (Fig. 13). These results suggested that the cell proliferation inhibition by amide-type SNIPER (**6**) is specific for neuroblastoma cells expressing MycN.

With regard to caspase activation and cell proliferation, ester-type SNIPER (**4**), as well as the combination of amide-type SNIPER

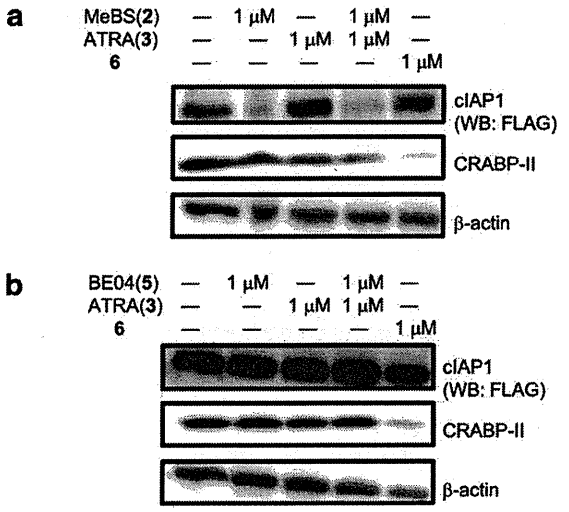

Figure 9. (a) Influence of combination of MeBS (**2**) and ATRA (**3**). Western blot-detection of CRABP-II and cIAP1 levels in HT1080 cells expressing FLAG-tagged cIAP1. The cells were treated with 1 μM MeBS (**2**), 1 μM ATRA (**3**), or 1 μM **6** for 6 h. (b) Influence of combination of BE04 (**5**) and ATRA (**3**). Western blot-detection of CRABP-II and cIAP1 levels in HT1080 cells expressing FLAG-tagged cIAP1. The cells were treated with 1 μM BE04 (**2**), 1 μM ATRA (**3**), or 1 μM **6** for 6 h. SNIPER (**6**) induced a decrease of CRABP-II, whereas the mixture of MeBS (**2**) or BE04 (**5**) and ATRA (**3**) did not. The treatments with MeBS (**2**) or BE04 (**5**), and the combination of MeBS (**2**) or BE04 (**5**) and ATRA (**3**) did not affect the CRABP-II level in HT1080. ATRA (**3**) did not cause any decrease of cIAP1 or CRABP-II. Thus, single treatment of HT1080 cells expressing FLAG-tagged cIAP1 with BE04 (**5**) and ATRA (**3**), which are partial structures of SNIPER (**6**), or their combination, did not induce degradation of CRABP-II.

(**6**) and MeBS (**2**), showed a stronger effect than amide-type SNIPER (**6**) alone (Figs. 11c and 14), even though **4** and **6** equally decreased CRABP-II and MycN (Fig. 11a and b). These results suggested that down-regulation of both cIAP1 and CRABP-II is more effective than down-regulation of CRABP-II alone to inhibit cell growth and induce apoptosis of neuroblastoma cells. This discovery was made possible by the development of CRABP-II-specific amide-type SNIPER (**6**).

4. Conclusion

In conclusion, the previously reported ester-type SNIPER induces degradation of not only its target protein, but also cIAP1, and therefore in the present work we designed amide-type SNIPER to improve the target protein/cIAP1 degradation selectivity. We synthesized the designed amide-type SNIPER, and confirmed that it does indeed shows improved selectivity. This is an interesting example illustrating that modification of just one atom of a bioactive molecule can cause a major change of activity. We also confirmed that amide-type SNIPER is an effective chemical tool to study the involvement of CRABP-II in MycN-mediated caspase activation in living neuroblastoma cells, finding that: (i) degradation of CRABP-II induces caspase activation and inhibits proliferation of neuroblastoma cells, (ii) degradation of both CRABP-II and cIAP1 is more effective than down-regulation of CRABP-II alone to inhibit the cell proliferation. Amide-type SNIPER should be adaptable to various other target proteins by using appropriate specific ligands, and we are currently examining protein knockdown of other target proteins with amide-type SNIPERs. We believe that highly selective target protein knockdown with SNIPERs will provide new insights into the chemical biology of various proteins and open up new strategies for drug therapy.

5. Experimental section

5.1. Chemistry

Proton nuclear magnetic resonance spectra (^{1}H NMR) and carbon nuclear magnetic resonance spectra (^{13}C NMR) were recorded on a JEOL JNMGX500 (500 MHz) spectrometer in the indicated solvent. Chemical shifts (δ) are reported in parts per million relative to the internal standard tetramethylsilane. High-resolution mass spectra (HRMS) and fast atom bombardment (FAB) mass spectra were recorded on a JEOL JMA-HX110 mass spectrometer. Bestatin (**1**) and methyl bestatin (MeBS, **2**) were provided by Nippon Kayaku Co., Ltd (Tokyo, Japan). The other chemical reagents and solvents were purchased from Aldrich, Merck, Tokyo Kasei Kogyo, Wako Pure Chemical Industries, and Kanto Kagaku and used without purification. Flash column chromatography was performed

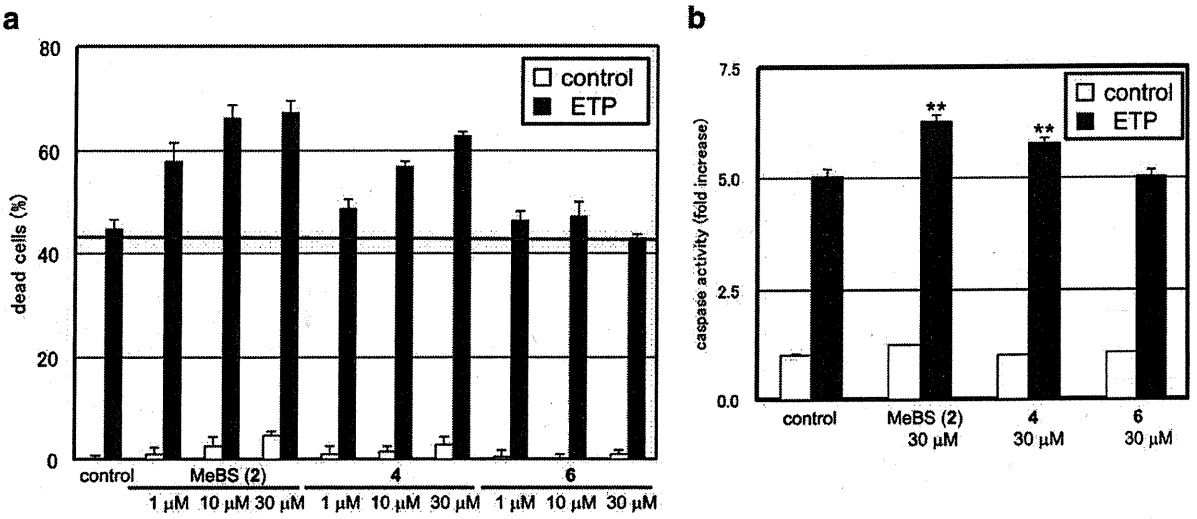

Figure 10. (a) LDH assay. HT1080 cells were treated with compounds in the presence or absence of 30 μg/mL etoposide (ETP) for 24 h. The data are the means of triplicate determinations. (b) Caspase activity assay. HT1080 cells were treated with compounds in the presence or absence of 30 μg/mL etoposide (ETP) for 24 h. The data are the means of triplicate determinations. $^{**}P < 0.01$; ANOVA and Bonferroni-type multiple t test results indicated significant differences between ETP control and the combination of ETP with MeBS (**2**), and between ETP control and the combination of ETP with **4**.

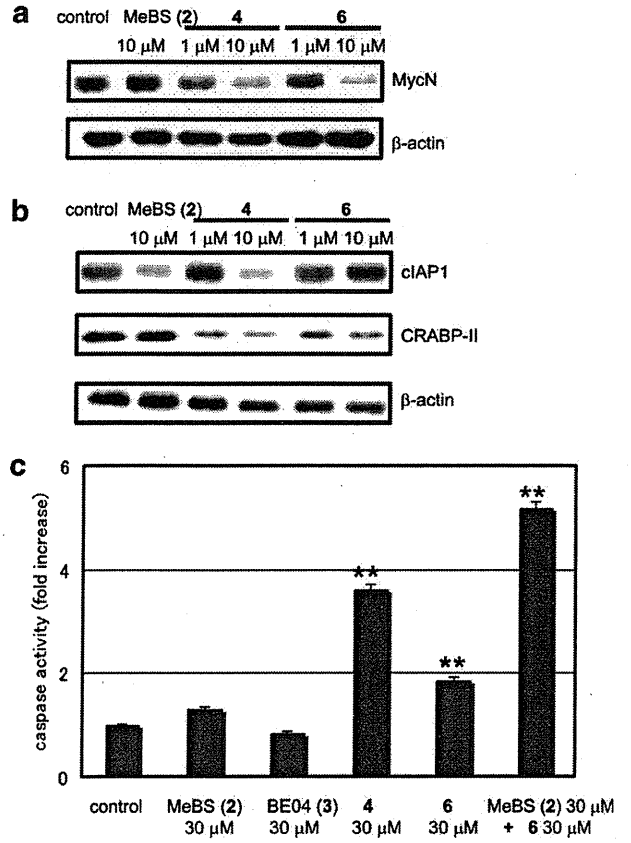

Figure 11. (a) Western blotting detection of MycN in IMR-32 cells. Western blot-detection of MycN levels in IMR-32 cells after 48-h treatment with MeBS (**2**), **4**, and **6**. (b) Western blot-detection of cIAP1 and CRABP-II levels in IMR-32 cells after 24-h treatment with MeBS (**2**), SNIPER (**4**), and SNIPER (**6**). (c) Caspase activity assay. IMR-32 cells were treated with compounds for 24 h. The data are the means of triplicate determinations. $^{**}P < 0.01$; ANOVA and Bonferroni-type multiple *t* test results indicated significant differences from the control for **4**, **6** and the combination of MeBS (**2**) with **6**.

using Silica Gel 60 (particle size 0.060–0.210 mm) supplied by Kanto Kagaku.

5.1.1. (*S*)-Methyl 4-methyl-2-(4-phenylbutanamido)pentanoate (12)

EDCI (2.61 g, 13.6 mmol) was added to a solution of leucine methyl ester hydrochloride (**10**) (2.45 g, 13.5 mmol), 4-phenylbutanoic acid (**11**) (1.50 g, 9.14 mmol), $HOBt{\cdot}H_2O$ (2.86 g, 18.7 mmol) and Et_3N (5.60 mL, 40.4 mmol) in THF (150 mL) with cooling in an ice-bath. The resulting mixture was stirred at room temperature for 5 h, then concentrated, and the residue was extracted with AcOEt. The organic solution was washed with 10% aqueous citric acid, saturated $NaHCO_3$ and brine, and dried over Mg_2SO_4. Filtration and evaporation of the solvent in vacuo gave 2.65 g (100%) of **12** as a colorless oil; ^{1}H NMR ($CDCl_3$, 500 MHz, δ; ppm): 7.30–7.16 (5H, m), 5.74 (1H, br d, J = 7.3 Hz), 4.65 (1H, m), 3.73 (3H, s), 2.66 (2H, t, J = 7.3 Hz), 2.21 (2H, t, J = 7.3 Hz), 1.98 (2H, quin, J = 7.3 Hz), 1.54 (3H, m), 0.94 (3H, d, J = 5.7 Hz), 0.93 (3H, d, J = 5.7 Hz); MS (FAB) *m/z*: 292 (MH^+).

5.1.2. Preparation of (*S*)-2-[(2*S*,3*R*)-3-(*tert*-butoxycarbonyl)-2-hydroxy-4-phenylbutanamido]-4-methylpentanoic acid (*N*-Boc bestatin, 13)

To a suspension of bestatin (**1**) (950 mg, 3.08 mmol) in acetone (140 mL) was added 2 N aqueous NaOH (3.10 mL, 6.20 mmol) and $(Boc)_2O$ (1.40 g, 6.41 mmol) with cooling in an ice-bath. The resulting mixture was stirred at room temperature for 24 h, then concentrated in vacuo, and the residue was dissolved in AcOEt. The organic solution was washed with 10% aqueous citric and brine, and dried over $MgSO_4$. Filtration, evaporation of the solvent in vacuo and purification of the residue by flash column chromatography (AcOEt/*n*-hexane = 1:2 to AcOEt only) gave 770 mg (61%) of **13** as a colorless solid; ^{1}H NMR (DMSO-d_6, 500 MHz, δ; ppm); 7.74 (1H, d, J = 8.5 Hz), 7.27–7.16 (5H, m), 6.12 (1H, d, J = 9.3 Hz), 6.02 (1H, m), 4.28 (1H, m), 3.90 (1H, m), 3.82 (1H, m), 2.78 (1H, dd, J = 13.1, 7.0 Hz), 2.63 (1H, dd, J = 13.1, 7.9 Hz), 1.64–1.59 (2H, m), 1.47 (1H, m), 1.27 (9H, s), 0.86 (3H, d, J = 6.0 Hz), 0.81 (3H, d, J = 6.1 Hz); MS (FAB) *m/z*: 431 (MNa^+), 409 (MH^+).

5.1.3. (*R*)-2-Isobutyl-4-oxo-7-phenylheptanoic acid (14)

$LiOH{\cdot}H_2O$ (823 mg, 19.6 mmol) was added to a solution of **12** (2.48 g, 8.51 mmol) in $MeOH/H_2O$ (60.0 mL/30.0 mL) and the resulting mixture was stirred at room temperature for 15 h. Then the reaction mixture was acidified with 2 N HCl and concentrated in vacuo. The residue was extracted with AcOEt. The organic solution was washed with brine, and dried over Mg_2SO_4. Filtration and evaporation of the solvent in vacuo gave a crude solid, which was suspended in AcOEt. Insoluble material was collected by filtration to give 2.20 g (93%) of **14** as a colorless solid; ^{1}H NMR (DMSO-d_6, 500 MHz, δ; ppm): 12.43 (1H, br), 8.04 (1H, d, J = 7.9 Hz), 7.26 (2H, t, J = 7.9 Hz), 7.16 (3H, m), 4.21 (1H, m), 2.54 (2H, t, J = 7.3 Hz), 2.12 (2H, d, J = 7.3 Hz), 1.75 (2H, quin, J = 7.3 Hz), 1.63 (1H, m), 1.49 (2H, m), 0.87 (3H, d, J = 6.7 Hz), 0.83 (3H, d, J = 6.7 Hz); MS (FAB) *m/z*: 278 (MH^+).

5.1.4. *tert*-Butyl (2*R*,3*S*)-3-hydroxy-4-[(*S*)-4-methyl-1-(methylamino)-1-oxopentan-2-ylamino]-4-oxo-1-phenylbutan-2-ylcarbamate (15)

EDCI (72.0 mg, 0.376 mmol) was added to a solution of **14** (104 mg, 0.255 mmol), methylamine hydrochloride (75.0 mg, 1.11 mmol), $HOBt{\cdot}H_2O$ (78.0 mg, 0.509 mmol) and iPr_2NEt (220 μL, 1.26 mmol) in DMF/CH_2Cl_2 (4.00 mL/3.00 mL) with cooling in an ice-bath. The resulting mixture was stirred at room temperature for 22 h, then quenched with water, and extracted with AcOEt. The organic layer was washed with brine, and dried over $MgSO_4$ Filtration, evaporation of the solvent in vacuo and purification of the residue by flash column chromatography (AcOEt only) gave 94.0 mg (88%) of **15** as a colorless solid; ^{1}H NMR ($CDCl_3$, 500 MHz, δ; ppm): 7.29 (2H, t, J = 6.7 Hz), 7.23 (3H, m), 6.97 (1H, d, J = 8.5 Hz), 6.36 (1H, br), 5.44 (1H, d, J = 4.9 Hz), 4.98 (1H, d, J = 7.9 Hz), 4.44 (1H, m), 4.11 (2H, dd, J = 7.3, 3.0 Hz), 4.00 (1H, m), 3.11 (1H, m), 3.04 (1H, m), 2.78 (1.5H, s), 2.77 (1.5H, s), 1.65 (3H, m), 1.39 (9H, s), 0.93 (3H, d, J = 6.0 Hz), 0.89 (3H, d, J = 6.1 Hz); MS (FAB) *m/z*: 444 (MNa^+), 422 (MH), 322 (MH^+–Boc).

5.1.5. (*S*)-2-[(2*S*,3*R*)-3-Amino-2-hydroxy-4-phenylbutanamido]-*N*,4-dimethylpentanamide hydrochloride (BE04, 5)

4 N HCl in 1,4-dioxane (500 μL, 2.00 mmol) was added to **15** (63.2 mg, 0.150 mmol) in CH_2Cl_2 (1.00 mL) with cooling in an ice-bath and the resulting mixture was stirred at room temperature for 2 h, then concentrated in vacuo to give 53.2 mg (99%) of **5** as a colorless solid; ^{1}H NMR (DMSO-d_6, 500 MHz, δ; ppm): 8.04–7.97 (5H, m), 7.34–7.23 (5H, m), 6.66 (1H, d, J = 6.1 Hz), 4.22 (1H, m), 3.99 (1H, m), 3.53 (1H, br), 2.95–2.82 (2H, m), 2.54 (1.5H, s), 2.53 (1.5H, s), 1.52–1.42 (3H, m), 0.87 (3H, d, J = 6.1 Hz), 0.84 (3H, d, J = 6.7 Hz); ^{13}C NMR ($CDCl_3$, 125 MHz, δ; ppm): 171.97, 170.64, 136.27, 129.44, 128.65, 126.94, 68.18, 54.20, 51.24, 40.92, 34.70, 25.55, 24.24, 22.85, 21.91; MS (FAB) *m/z*: 322 (MH^+); HRMS (FAB) calcd for $C_{17}H_{28}N_3O_3^+$, 322.2131; found 322.2115.

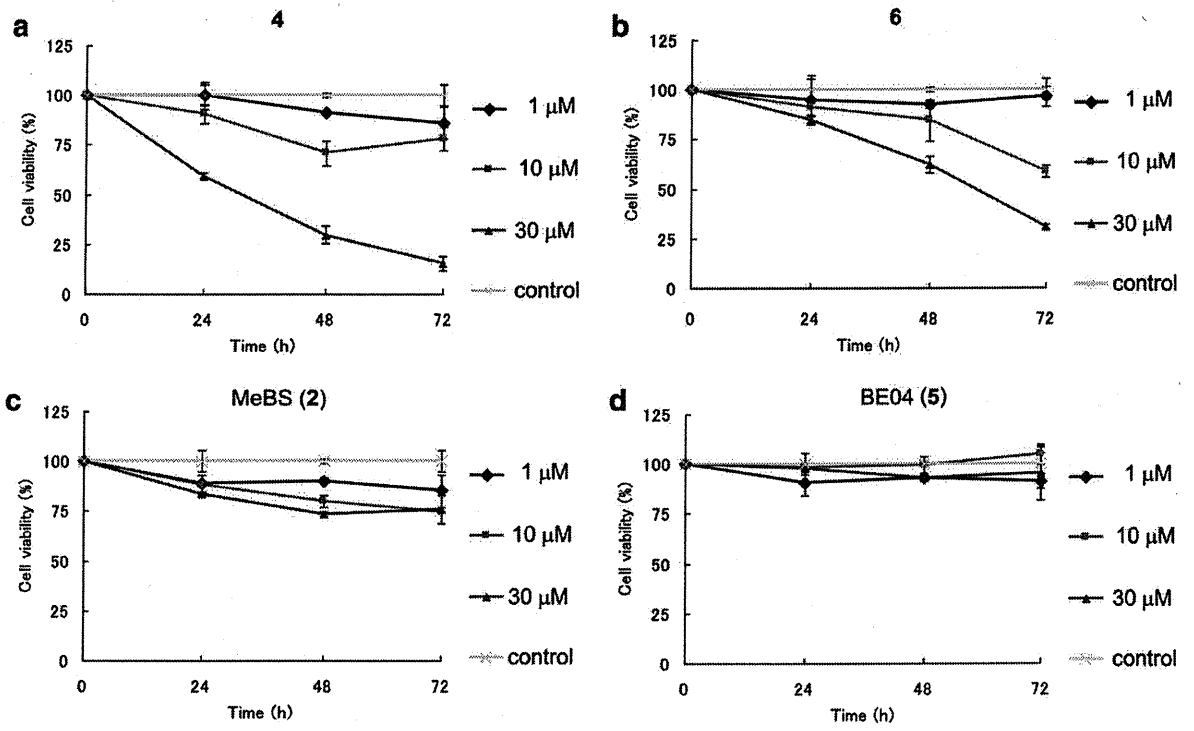

Figure 12. Viability of IMR-32 cells treated with (a) **4**, (b) **6**, (c) MeBS (**2**), and (d) BE04 (**5**).

5.1.6. (*S*)-*N*,4-Dimethyl-2-(4-phenylbutanamido)pentanamide (7)

Compound **7** (yield; 106 mg, 99%) was prepared from **14** (102 mg, 0.368 mmol), methylamine hydrochloride (134 mg, 1.98 mmol) using the procedure described for **15**; yellow solid; ^{1}H NMR ($CDCl_3$, 500 MHz, δ; ppm): 7.28 (2H, t, J = 7.3 Hz), 7.21 (1H, d, J = 7.3 Hz), 7.17 (2H, d, J = 7.3 Hz), 6.10 (1H, br), 5.83 (1H, d, J = 8.5 Hz), 4.41 (1H, m), 2.80 (1.5H, s), 2.79 (1.5H, s), 2.63 (2H, t, J = 7.6 Hz), 2.20 (2H, t, J = 7.3 Hz), 1.95 (2H, quin, J = 7.6 Hz), 1.66–1.49 (3H, m), 0.93 (3H, d, J = 5.4 Hz), 0.92 (3H, d, J = 6.0 Hz); ^{13}C NMR ($CDCl_3$, 125 MHz, δ; ppm): 173.02, 172.75, 141.49, 128.68, 128.63, 126.29, 51.64, 41.24, 35.90, 35.32, 27.19, 26.49, 24.96, 23.04, 22.43; MS (FAB) *m/z*: 291 (MH^+); HRMS (FAB) calcd for $C_{17}H_{27}N_2O_2^+$, 291.2073; found 291.2076.

5.1.7. 5-(Dimethylamino)-*N*-(2-hydroxyethyl)naphthalene-1-sulfonamide (19)

2-Aminoethanol (**18**) (250 μL, 4.14 mmol) was added to a solution of 5-(dimethylamino)naphthalene-1-sulfonyl chloride (**17**) (216 mg, 0.801 mmol) and Et_3N (600 μL, 4.33 mmol) in CH_2Cl_2, (20.0 mL) with cooling by an ice-bath and the resulting mixture was stirred at room temperature for 2 h, then poured into water. The organic layer was washed with brine and dried over Mg_2SO_4. Filtration, evaporation of the solvent in vacuo and purification of the residue by flash column chromatography (CH_2Cl_2/MeOH = 10:1) gave 160 mg (68%) of **19** as a fluorescent powder; ^{1}H NMR ($CDCl_3$, 500 MHz, δ; ppm): 8.55 (1H, d, J = 8.5 Hz), 8.28 (1H, d, J = 8.5 Hz), 8.26 (1H, d, J = 7.3 Hz), 7.58 (1H, t, J = 8.2 Hz), 7.53 (1H, t, J = 7.3 Hz), 7.20 (1H, d, J = 7.3 Hz), 5.20 (1H, br d, J = 7.3 Hz), 3.60 (2H, q, J = 4.8 Hz), 3.04 (2H, q, J = 5.9 Hz), 2.89 (6H, s), 1.89 (1H, br); MS (FAB) *m/z*: 294 (M^+).

5.1.8. (*S*)-2-[1-(Dimethylamino)naphthalene-5-sulfonamido]ethyl 2-[(2*S*,3*R*)-3-(*tert*-butoxycarbonyl)-2-hydroxy-4-phenylbutanamido]-4-methylpentanoate (20)

Compound **20** (yield; 83.2 mg, 24%) was prepared from *N*-Boc bestatin (**13**) (202 mg, 0.495 mmol) and alcohol **19** (108 mg, 0.367 mmol) using the procedure described for **15**; fluorescent solid; ^{1}H NMR ($CDCl_3$, 500 MHz, δ; ppm): 8.55 (1H, d, J = 8.5 Hz), 8.28 (1H, d, J = 8.5 Hz), 8.22 (1H, dd, J = 7.0, 1.2 Hz), 7.53 (1H, t, J = 7.8 Hz), 7.50 (1H, t, J = 7.3 Hz), 7.35–7.15 (6H, m), 5.83 (1H, m), 5.45 (1H, m), 5.17 (1H, br d, J = 6.7 Hz), 4.40 (1H, m), 4.20–4.12 (2H, m), 4.11–4.05 (2H, m), 3.25–3.00 (4H, m), 2.89 (6H, s), 1.63–1.52 (3H, m), 1.37 (9H, s), 0.91 (3H, d, J = 6.1 Hz), 0.89 (3H, d, J = 6.1 Hz); MS (FAB) *m/z*: 684 (M^+), 585 (MH^+–Boc).

5.1.9. (*S*)-2-[1-(Dimethylamino)naphthalene-5-sulfonamido]ethyl 2-[(2*S*,3*R*)-3-amino-2-hydroxy-4-phenylbutanamido]-4-methylpentanoate dihydrochloride (DanBE·2HCl, 16·2HCl)

Compound **9**·2HCl (yield; 42.6 mg, 100%) was prepared from **20** (44.6 mg, 0.0651 mmol) using the procedure described for **5**; fluorescent powder; ^{1}H NMR (DMSO-d_6, 500 MHz, δ; ppm): 8.66 (1H, br d, J = 8.5 Hz), 8.43 (1H, br d, J = 7.9 Hz), 8.31 (2H, m), 8.13 (1H, d, J = 6.7 Hz), 8.04 (3H, br), 7.68 (1H, t, J = 7.9 Hz), 7.66 (1H, t, J = 7.3 Hz), 7.54 (1H, br), 7.30–7.20 (5H, m), 4.22 (1H, m), 4.00 (1H, d, J = 3.6 Hz), 3.93 (2H, m), 3.49 (1H, m), 3.06–2.82 (10H, m), 1.65–1.40 (3H, m), 0.86 (3H, d, J = 6.1 Hz), 0.82 (3H, d, J = 6.1 Hz); ^{13}C NMR (DMSO-d_6, 125 MHz, δ; ppm) 171.89, 171.12, 136.36, 136.21, 129.42, 128.88, 128.84, 128.58, 128.32, 128.09, 127.78, 126.86, 124.39, 68.26, 66.34, 63.34, 54.27, 50.39, 45.49, 41.12, 34.50, 24.16, 22.65, 21.54; MS (FAB) *m/z*: 585 (MH^+); HRMS (FAB) calcd for $C_{30}H_{41}N_4O_6S^+$, 585.2747; found 585.2727.

5.1.10. *tert*-Butyl 2-[2-(2-azidoethoxy)ethoxy]ethylcarbamate (22)

A mixture of *p*-toluenesulfonyl chloride (583 mg, 3.06 mmol) in CH_2Cl_2 (20.0 mL) was added to a solution of **21**[1] (380 mg, 1.52 mmol), Et_3N (500 μL, 3.61 mmol) and DMAP (37.0 mg, 0.303 mmol) CH_2Cl_2 (2.00 mL) in a dropwise fashion over a period of 1 h. The resulting mixture was stirred at room temperature for 1 h, then poured into water. The organic layer was washed with brine, and dried over $MgSO_4$. Filtration, evaporation of the solvent

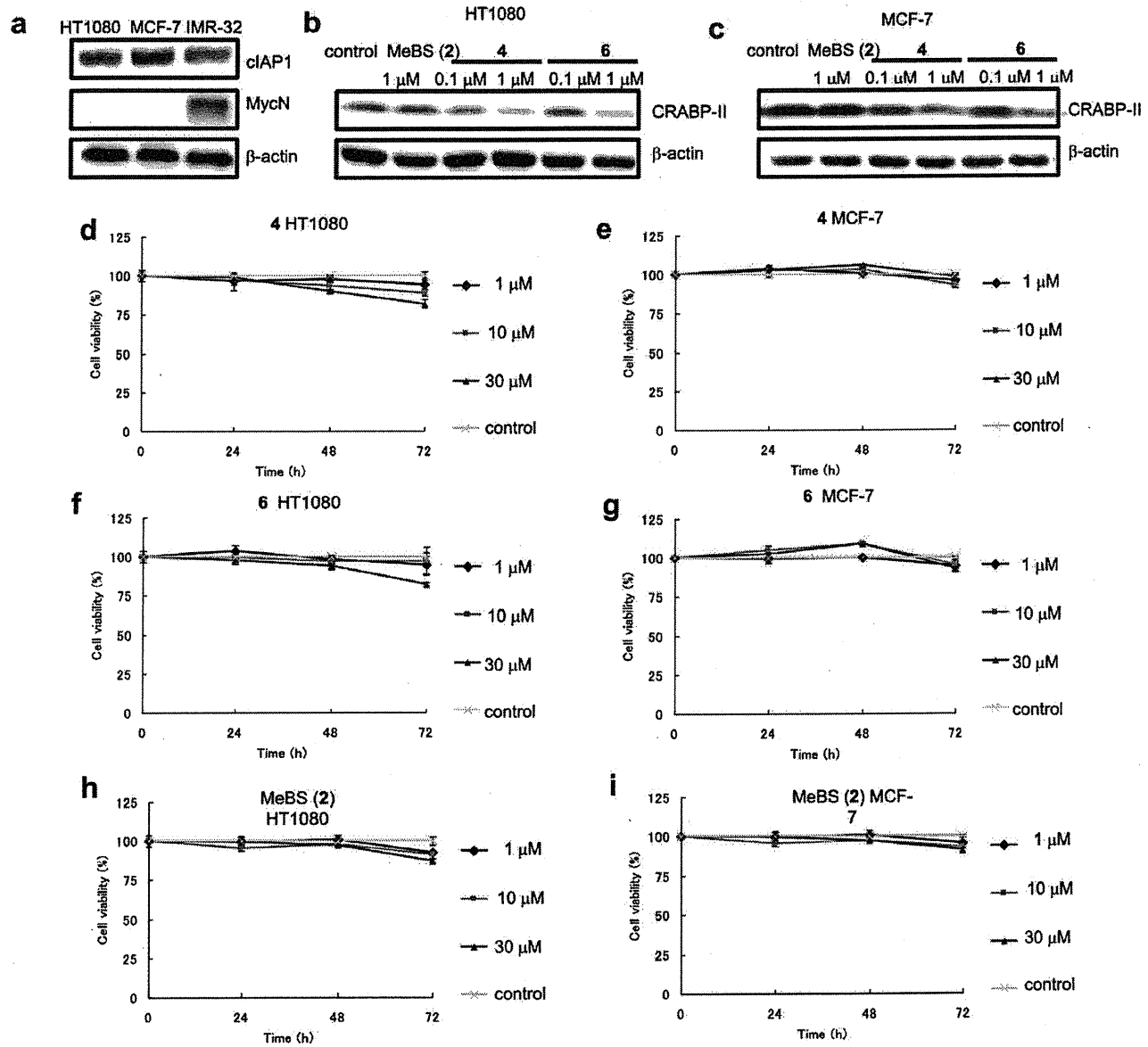

Figure 13. (a) Western blot-detection of cIAP1 and MycN levels in HT1080 cells, MCF-7 cells and IMR-32 cells. (b) Western blot-detection of CRABP-II levels in HT1080 cells after 6-h treatment with MeBS (**2**), ester-type SNIPER (**4**) and amide-type SNIPER (**6**). (c) Western blot-detection of CRABP-II levels in MCF-7 cells after 24-h treatment with MeBS (**2**), ester-type SNIPER (**4**), and amide-type SNIPER (**6**). (d–i) Viability of HT1080 and MCF-7 cells treated with MeBS (**2**), ester-type SNIPER (**4**) and amide-type SNIPER (**6**).

in vacuo and purification of the residue by flash column chromatography (AcOEt/*n*-hexane = 1:1 AcOEt only) gave 515 mg (84%) of **22** as a colorless oil. A suspension of **22** (500 mg, 1.24 mmol) and NaN_3 (180 mg, 2.77 mmol) in DMF (5.00 mL) was stirred at 60 °C for 8 h. Then, the reaction mixture was poured into water and extracted with AcOEt. The organic layer was washed with brine, and dried over $MgSO_4$. Filtration and evaporation of the solvent in vacuo gave 335 mg (98%) of **23** as a colorless oil; ^1H NMR ($CDCl_3$, 500 MHz, δ; ppm): 5.01 (1H, br), 3.69 (6H, m), 3.56 (2H, t, J = 4.9 Hz), 3.41 (2H, t, J = 7.5 Hz), 3.32 (2H, m); 1.44 (9H, s); MS (FAB) *m/z*: 297 (MNa^+), 275 (MH^+), 175 (MH^+–Boc).

5.1.11. *tert*-Butyl 2-(2-(2-aminoethoxy)ethoxy)ethylcarbamate (24)

10% Pd/C (20.2 mg) was added to a solution of **23** (211 mg, 0.769 mmol) in EtOH (5.00 mL). After having been stirred at room temperature under H_2 for 13 h, the reaction mixture was filtered though Celite. The solvent was removed by concentration in vacuo to give crude **24** (191 mg) as a colorless oil, which was used in the next reaction without further purification; MS (FAB) *m/z*: 249 (MH^+).

5.1.12. (*S*)-2-{2-[2-(*tert*-Butoxycarbonyl)ethoxy]ethoxy}ethyl 2-((2*S*,3*R*)-3-{[(9*H*-fluoren-9-yl)methoxy]carbonyl}-2-hydroxy-4-phenyl-butanamido)-4-methylpentanamide (26)

Compound **26** (56.0 mg, 78%; from **25**) was prepared from crude amine (**24**) (140 mg) and **25**[2] (50.1 mg, 0.0944 mmol) using the procedure described for **15**; colorless oil; ^1H NMR ($CDCl_3$, 500 MHz, δ; ppm): 7.76 (2H, d, J = 7.3 Hz), 7.51 (2H, m), 7.38 (2H, t, J = 7.6 Hz), 7.31–7.14 (7H, m), 6.70 (1H, br), 5.80 (1H, br d, J = 6.1 Hz), 5.48 (1H, m), 5.43 (1H, m), 5.12 (1H, m), 4.48 (1H, m), 4.43–4.20 (5H, m), 3.54–3.40 (10H, m), 3.28 (2H, br q, J = 4.3 Hz),

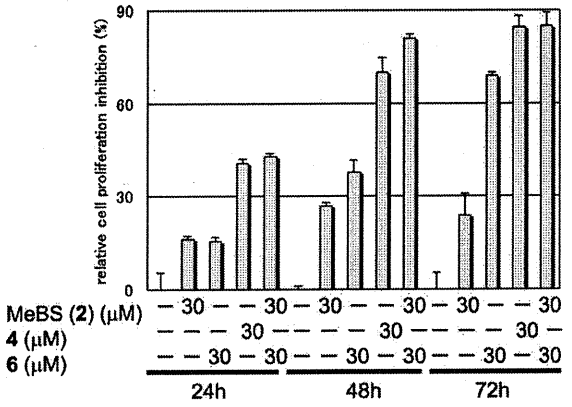

Figure 14. Relative inhibition of proliferation of IMR-32 cells by treatment with MeBS (**2**), SNIPER (**4**), SNIPER (**6**), and the combination of MeBS (**2**) and SNIPER (**6**). The graph was drawn based on calculated IMR-32 cells viability. SNIPER (**4**) or the combination of SNIPER (**6**) and MeBS (**2**) inhibited proliferation of IMR-32 cells more strongly than did SNIPER (**6**). The activity of the combination of SNIPER (**6**) and MeBS (**2**) was similar to that of SNIPER (**4**).

3.05 (2H, m), 1.62 (3H, m), 1.44 (9H, s), 0.93 (3H, d, J = 6.0 Hz), 0.89 (3H, d, J = 6.1 Hz); MS (FAB) m/z: 761 (MH^+), 661 (MH^+–Boc).

5.1.13. (*S*)-*tert*-Butyl 2-(2-{2-[4-methyl-2-(4-phenylbutanamido)pentanamido]ethoxy}ethoxy)ethylcarbamate (27)

Compound **27** (yield; 47.5 mg, 88%) was prepared from **14** (29.5 mg, 0.106 mmol) and crude amine (**24**) (50.0 mg) using the procedure described for **15**; colorless oil; ^{1}H NMR ($CDCl_3$, 500 MHz, δ; ppm): 7.27 (2H, t, J = 7.3 Hz), 7.18 (1H, t, J = 7.3 Hz), 7.17 (2H, d, J = 6.7 Hz), 6.65 (1H, m), 6.02 (1H, m), 5.20 (1H, m), 4.47 (1H, m), 3.76–3.44 (10H, m), 3.32 (2H, m), 2.63 (2H, t, J = 7.6 Hz), 2.21 (2H, t, J = 7.3 Hz), 1.95 (2H, quin, J = 7.6 Hz), 1.62 (2H, m), 1.59 (1H, m), 1.43 (9H, s), 0.93 (3H, d, J = 6.1 Hz); MS (FAB) m/z: 508 (MH^+), 408 (MH^+–Boc).

5.1.14. (9*H*-Fluoren-9-yl)methyl (2*R*,3*S*)-4-((*S*)-1-{2-[2-(2-aminoethoxy)ethoxy]ethylamino}-4-methyl-1-oxopentan-2-ylamino)-3-hydroxy-4-oxo-1-phenylbutan-2-ylcarbamate hydrochloride (29·HCl)

4 N HCl in 1,4-dioxane (250 μL, 1 mmol) was added to **26** (56.1 mg, 0.0736 mmol) with cooling in an ice-bath and the resulting mixture was stirred at room temperature for 1 h. The reaction mixture was concentrated in vacuo to give crude **29**·HCl (51.2 mg), which was used in the next step without further purification; MS (FAB) m/z: 661 (MH^+–HCl).

5.1.15. (*S*)-*N*-{2-[2-(2-Aminoethoxy)ethoxy]ethyl}-4-methyl-2-(4-phenylbutanamido)pentanamide hydrochloride (30·HCl)

Crude **30**·HCl was prepared from **27** (47.5 mg, 0.0936 mmol) using the procedure described for **29**·HCl. Crude **30**·HCl (45.3 mg) was used in next step without further purification.

5.1.16. (2*E*,4*E*,6*E*,8*E*)-2-Cyanoethyl 9-((*E*)-3-{2-[2-(2-{2-[(*S*)-2-((2*S*,3*R*)-3-{[(9*H*-fluoren-9-yl)methoxy]carbonyl}-2-hydroxy-4-phenyl butanamido)-4-methylpentanamido]ethoxy}ethoxy)ethylamino]-2-oxoethoxyimino}-2,6,6-trimethylcyclohex-1-enyl)-3,7-dimethylnona-2,4,6,8-tetraenoate (31)

Compound **31** (40.3 mg, 56% from **28**) was prepared from **28**[2] (29.2 mg, 0.0662 mmol) and crude **29**·HCl (51.2 mg) using the procedure described for **12**; yellow oil; ^{1}H NMR ($CDCl_3$, 500 MHz, δ; ppm): 7.72 (2H, d, J = 7.3 Hz), 7.46 (2H, d, J = 7.3 Hz), 7.35 (2H, t, J = 7.3 Hz), 7.34–7.22 (7H, m), 7.00 (1H, dd, J = 15.2, 11.0 Hz), 6.80 (1H, br), 6.66 (1H, m), 6.32–6.16 (4H, m), 5.78 (1H, s), 5.48 (1H, d, J = 8.5 Hz), 5.36 (1H, d, J = 5.5 Hz), 4.55 (2H, s), 4.36 (1H, m), 4.34 (7H, m), 3.60 (10H, m), 3.37 (2H, m), 2.98 (2H, m), 2.70 (2H, t, J = 6.1 Hz), 2.63 (2H, t, J = 6.4 Hz), 2.33 (3H, s), 2.01 (3H, s), 1.83 (3H, s), 1.67 (1H, m),1.58 (4H, m), 1.06 (6H, s), 0.84 (3H, d, J = 6.0 Hz), 0.81 (3H, d, J = 6.1 Hz); MS (FAB) m/z: 1083 (M^+).

5.1.17. (2*E*,4*E*,6*E*,8*E*)-2-Cyanoethyl 3,7-dimethyl-9-((*E*)-2,6,6-trimethyl-3-{2-[2-(2-{2-[(*S*)-4-methyl-2-(4-phenylbutanamido)pentanamido]ethoxy}ethoxy)ethylamino]-2-oxoethoxyimino}cyclohex-1-enyl)nona-2,4,6,8-tetraenoate (32)

Compound **32** (yield; 23.2 mg, 62% from **28**) was prepared from **28** (20.0 mg, 0.454 mmol) and crude **30**·HCl (45.3 mg) using the procedure described for **12**; yellow solid; ^{1}H NMR ($CDCl_3$, 500 MHz, δ; ppm): 7.27 (2H, t, J = 7.3 Hz), 7.19 (1H, t, J = 7.3 Hz), 7.16 (2H, d, J = 7.3 Hz), 7.03 (1H, dd, J = 14.6, 11.6 Hz), 6.68 (1H, br), 6.57 (1H, br), 6.36–6.20 (4H, m), 5.82 (1H, s), 4.58 (2H, s), 4.45 (1H, m), 4.33 (2H, t, J = 6.1 Hz), 3.59–3.40 (12H, m), 2.73 (2H, t, J = 6.1 Hz), 2.66 (4H, m), 2.37 (3H, s), 2.21 (2H, t, J = 7.3 Hz), 2.03 (3H, s), 1.95 (2H, quin, J = 7.9 Hz), 1.86 (3H, S), 1.68–1.54 (5H, m), 1.09 (6H, s), 0.93 (3H, d, J = 2.4 Hz), 0.92 (3H, d, J = 2.4 Hz); MS (FAB) m/z: 830 (MH^+).

5.1.18. (2*E*,4*E*,6*E*,8*E*)-9-[(*E*)-3-(2-{2-[2-(2-{(*S*)-2-[(2*S*,3*R*)-3-Amino-2-hydroxy-4-phenylbutanamido]-4-methylpentanamido}ethoxy)ethoxy]ethylamino}-2-oxoethoxyimino)-2,6,6-trimethylcyclohex-1-enyl]-3,7-dimethylnona-2,4,6,8-tetraenoic acid (amide-type SNIPER, 6)[2–4]

1 N TBAF in THF (370 μL, 0.370 mmol) was added to a solution of **31** (40.3 mg, 0.0372 mmol) and MeOH (30.0 μL, 0.741 mmol). After having been stirred at room temperature for 1 h, the mixture was purified by flash column chromatography ($CHCl_3$/MeOH = 20:1) to give 33 mg of crude acid as a yellow oil. DBU (17.0 μL, 0.114 mmol) was added to a solution of the crude acid and dodecyl mercaptan (13.0 μL, 0.0552 mmol) in CH_2Cl_2 (1.00 mL). After having been stirred at room temperature for 1 h, the mixture was purified by flash column chromatography ($CHCl_3$/MeOH = 9:1) and PTLC ($CHCl_3$/MeOH/NH_3 aqueous = 3:1:0.1) to give 17.2 mg (57%; two steps) of **6** as a yellow oil; ^{1}H NMR ($CDCl_3$, 500 MHz, δ; ppm): 7.87 (1H, d, J = 6.7 Hz), 7.30–7.24 (5H, m), 7.01 (1H, m), 6.97 (1H, dd, J = 15.2, 12.1 Hz), 6.73 (1H, s), 6.38–6.18 (4H, m), 5.82 (1H, s), 4.58 (2H, s), 4.44 (1H, m), 4.07 (1H, m), 3.72–3.50 (13H, m), 3.33 (2H, m), 3.02 (2H, m), 2.66 (2H, t, J = 6.7 Hz), 2.33 (3H, s), 2.02 (3H, s), 1.86 (3H, s), 1.67 (5H, m), 1.09 (6H, s), 0.93 (3H, d, J = 6.1 Hz), 0.92 (3H, d, J = 6.0 Hz); ^{13}C NMR ($CDCl_3$, 125 MHz, δ; ppm): 173.34, 172.02, 170.67, 158.88, 150.34, 139.35, 138.38, 138.06, 136.72, 131.64, 129.34, 128.75, 126.74, 126.61, 124.79, 73.03, 70.32, 70.21, 69.92, 69.76, 54.64, 51.84, 40.63, 39.31, 38.80, 35.97, 34.88, 27.62, 24.88, 23.02, 21.73, 20.23, 14.91, 13.86, 12.82; MS (FAB) m/z: 808 (MH^+); HRMS (FAB) calcd for $C_{44}H_{66}N_5O_9^+$, 808.4861; found 808.4825.

5.1.19. (2*E*,4*E*,6*E*,8*E*)-3,7-Dimethyl-9-((*E*)-2,6,6-trimethyl-3-{2-[2-(2-{2-[(*S*)-4-methyl-2-(4-phenylbutanamido)pentanamido]ethoxy}ethoxy)ethylamino]-2-oxoethoxyimino}cyclohex-1-enyl)nona-2,4,6,8-tetraenoic acid (8)

1 N TBAF in THF (280 μL, 0.280 mmol) was added to a solution of **32** (23.2 mg, 0.0279 mmol) and MeOH (22.0 μL, 0.543 mmol) in THF (560 μL). The mixture was stirred at room temperature for 2 h, then purified by flash column chromatography ($CHCl_3$ only to $CHCl_3$/MeOH = 20:1) and PTLC ($CHCl_3$/MeOH = 20:1) to give 15.1 mg (70%) of **8** as a yellow oil; ^{1}H NMR ($CDCl_3$, 500 MHz, δ;

ppm): 7.25 (2H, t, J = 7.3 Hz), 7.17 (1H, t, J = 7.3 Hz), 7.14 (2H, d, J = 6.7 Hz), 7.01 (1H, dd, J = 15.2, 11.6 Hz), 6.68 (1H, br), 6.61 (1H, br), 6.35–6.17 (4H, m), 5.82 (1H, s), 4.56 (2H, s), 4.45 (1H, m), 3.89–3.32 (12H, m), 2.65–2.58 (4H, m), 2.34 (3H, s), 2.20 (2H, t, J = 6.7 Hz), 2.00 (3H, s), 1.93 (2H, quin, J = 7.3 Hz), 1.84 (3H, S), 1.59–1.47 (5H, m), 1.07 (6H, s), 0.93 (3H, d, J = 6.1 Hz), 0.92 (3H, d, J = 6.1 Hz); ^{13}C NMR ($CDCl_3$, 125 MHz, δ; ppm): 172.84, 172.43, 170.47, 169.97, 158.76, 154.31, 150.15, 141.40, 139.21, 138.90, 136.25, 131.44, 131.06, 128.47, 128.39, 126.89, 125.98, 124.92, 118.32, 73.08, 70.40, 70.21, 69.91, 69.69, 51.55, 41.51, 39.29, 38.76, 35.99, 35.18, 34.87, 27.62, 27.11, 24.80, 22.88, 22.15, 20.22, 14.87, 13.95, 12.85; MS (FAB) m/z: 777 (MH^+); HRMS (FAB) calcd for $C_{44}H_{65}N_4O_8^+$, 777.4802; found 777.4843.

5.2. Biology

5.2.1. Cell culture conditions

Human fibrosarcoma HT1080 cells were cultured in RPMI 1640 containing 10% heat-inactivated fetal bovine serum (FBS), penicillin, and streptomycin mixture at 37 °C in a humidified atmosphere of 5% CO_2 in air. Human neuroblastoma IMR-32 cells were cultured in Eagle's minimal essential medium with non-essential amino acids and 10% FBS at 37 °C in a humidified atmosphere of 5% CO_2 in air. Human embryonic kidney (HEK) 293 cells and human mammary tumor MCF-7 cells were cultured in D-MEM medium containing 5% FBS and 10% FBS, respectively, at 37 °C in a humidified atmosphere of 5% CO_2 in air.

5.2.2. FLAG-IAPs transfection

The transfection experiments were carried out according to the method reported in Ref. 6.

5.2.3. Western blotting

HT1080, FLAG-IAPs HT1080, IMR-32 and MCF-7 (1×10^6) cells were treated for the indicated period with MeBS (**2**) (Nippon Kayaku Co., Ltd), ATRA (**3**) (Tokyo Kasei Kogyo), MG132 (Peptide Institute Inc.), lactacystin (Toronto Research Chemicals Inc.) and/or synthetic compounds at the indicated concentrations in an appropriate cell culture medium supplemented with 10% FBS, then the cells were collected and extracted with SDS buffer. Protein concentrations of the lysates were determined using a BCA protein assay. Equivalent amounts of protein from each lysate were resolved in 10–20% SDS–polyacrylamide gels and transferred onto PVDF membranes. After blocking with TBS containing 5% skim milk, the transblotted membranes were probed with rabbit polyclonal CRABP-II antibody (Novus Biologicals, Inc.) (1:1000 dilution), affinity-purified goat cIAP1 antibody (R&D systems) (0.5 μg/mL), mouse monoclonal RARα antibody (Perseus Proteomics Inc.) (1:1000 dilution), rabbit MycN antibody (Cell Signal Technology) (1:1000 dilution), anti-goat IgG-horseradish peroxidase conjugates (Kirkegaard & Perry Laboratories, Inc.) (1:5000 dilution), anti-mouse IgG-horseradish peroxidase conjugates (Chemicon) (1:2000 dilution), goat anti-rabbit IgG-horseradish peroxidase conjugates (Amersham) (1:2000 dilution), FLAG antibody (Sigma) (1:500 dilution), β-actin antibody (Santa Cruz Biotechnology, Inc.) (1:2000 dilution) in can-get-signal solution (Toyobo). After probing, the membrane was washed twice more with TBS-T. The immunoblots were visualized by enhanced chemiluminescence with Immobilon™ Western Chemiluminescent HRP Substrate (Millipore).

5.2.4. Binding assay

Recombinant GST-BIR3 and GST were produced and purified as described previously.[10] Serial dilutions of GST-BIR3 or GST were incubated in the presence of DanBE (1 μM) at room temperature for 5 min in phosphate-buffered saline (PBS, pH 7.4). After incubation, the fluorescence polarization of DanBE was measured on fluorescence spectrometer (Jasco FP-6500; excitation at 335 nm, emission at 550 nm). In competitive displacement studies, MeBS (**2**), BE04 (**5**) or compound **7** was incubated with GST-BIR3 for 5 min before the addition of DanBE.

5.2.5. Pull down assay

Pull down assays were carried out according to the method reported in Ref. 3.

5.2.6. Reporter gene assay

Reporter gene assays were carried out according to the method reported in Ref. 3.

5.2.7. Cell death assay

Etoposide was purchased from Sigma–Aldrich Corporation. CytoTox 96® Non-Radioactive Cytotoxicity Assay (Promega) was used for cell death assay. HT1080 cells were plated in 96-well plates at the initial density of 2×10^4 cells/well (50 μL/well) and incubated at 37 °C. After 24 h, cells were exposed to test compounds by adding solutions (50 μL/well) of the compounds at various concentrations in medium at 37 °C under 5% CO_2 in air for 24 h. Lysis buffer (15 μL) was added to high control wells and the plates were incubated at 37 °C for 45 min. Then 50 μL aliquots were taken from all wells using a multichannel pipette and transferred to fresh 96-well flat-bottomed (enzymatic assay) plates, and 50 μL of reconstituted Substrate Mix was added to each well of the enzymatic assay plate containing samples transferred from the cytotoxicity assay plate. The plates were incubated for 30 min at room temperature, then 50 μL of stop solution was added to each well and the absorbance at 490 nm in each well was measured with an ARVO™ SX microplate reader. The percentage cell growth was calculated from the absorbance readings.

5.2.8. Caspase assay

Apo-ONE® Homogeneous Caspase-3/7 Assay (Promega) was used for caspase assay. HT1080 and IMR-32 cells were plated in 96-well plates at the initial density of 2×10^4 cells/well (50 μL/well) and incubated at 37 °C. After 24 h, cells were exposed to test compounds by adding solutions (50 μL/well) of the compounds at various concentrations in medium at 37 °C under 5% CO_2 in air for 24 h. Then 100 μL of caspase activity detection reagent was added to each well. The plates were further incubated for 10 h (HT1080) or 0.5 h (IMR-32) at room temperature, and the fluorescence in each well was measured with an ARVO™ SX microplate reader (excitation at 485 nm, emission at 535 nm). The fold change of caspase activity was calculated from the fluorescence readings.

5.2.9. Cell proliferation inhibition assay

IMR-32, HT1080, and MCF-7 cells were plated in 96-well plates at the initial density of 2×10^4 cells/well (50 μL/well) and incubated at 37 °C. After 24 h, cells were exposed to test compounds by adding solutions (50 μL/well) of the compounds at various concentrations in medium at 37 °C under 5% CO_2 in air for 0–72 h. The mixtures were then treated with 10 μL of AlamarBlue® (Invitrogen), and incubation was continued at 37 °C for 3 h. The fluorescence in each well was measured with an ARVO™ SX microplate reader (excitation at 540 nm, emission, at 590 nm). The percentage cell growth was calculated from the fluorescence readings.

Acknowledgments

The work described in this paper was partially supported by Grants-in-Aid for Scientific Research from The Ministry of Education, Culture, Sports, Science and Technology, Japan and the Japan Society for the Promotion of Science. This work was also supported financially by the Takeda Science Foundation and the

Naito Foundation. We are grateful to Nippon Kayaku Co., especially Dr. Keiko Sekine, for providing bestatin (**1**) and MeBS (**2**), to Dr. Yukihide Tomari for help with Western blot-detection, and to Professor Makoto Makishima for providing RAR plasmids.

Supplementary data

Supplementary data (^{1}H NMR data) associated with this article can be found, in the online version, at doi:10.1016/j.bmc.2011.03.057.

References and notes

1. (a) Sakamoto, K. M.; Kim, K. B.; Kumagai, A.; Mercurio, F.; Crews, C. M.; Deshaies, R. J. *Proc. Natl. Acad. Sci. U.S.A.* **2001**, *98*, 8554; (b) Sakamoto, K. M.; Kim, K. B.; Verma, R.; Ransick, A.; Stein, B.; Crews, C. M.; Deshaies, R. J. *Mol. Cell. Proteomics* **2003**, *2*, 1350.
2. (a) Schneekloth, J. S.; Fonseca, F. M.; Koldobskiy, M.; Mandal, A.; Deshaies, R.; Sakamoto, S. M.; Crews, C. M. *J. Am. Chem. Soc.* **2004**, *126*, 3748; (b) Rodriguez-Gonzalez, A.; Cyrus, K.; Salcius, M.; Kim, K.; Crews, C. M.; Deshaies, R. J.; Sakamoto, K. M. *Oncogene* **2008**, *27*, 7201; (c) Puppala, D.; Lee, H.; Kim, K. B.; Swanson, H. I. *Mol. Pharmacol.* **2008**, *73*, 1064.
3. Itoh, Y.; Ishikawa, M.; Naito, M.; Hashimoto, Y. *J. Am. Chem. Soc.* **2010**, *132*, 5820.
4. Roy, N.; Deveraux, Q. L.; Takahashi, R.; Salvesen, G. S.; Reed, J. C. *EMBO J.* **1997**, *16*, 6914.
5. Vaux, D. L.; Silke, J. *Nat. Rev. Mol. Cell Biol.* **2005**, *6*, 287.
6. Sekine, K.; Takubo, K.; Kikuchi, R.; Nishimoto, M.; Kitagawa, M.; Abe, F.; Nishikawa, K.; Tsuruo, T.; Naito, M. *J. Biol. Chem.* **2008**, *283*, 8961.
7. Sato, S.; Aoyama, H.; Miyachi, H.; Naito, M.; Hashimoto, Y. *Bioorg. Med. Chem. Lett.* **2008**, *18*, 3354.
8. (a) Deveraux, Q. L.; Reed, J. C. *Gene Dev.* **1999**, *13*, 239; (b) Salvesen, G. S.; Duckett, C. S. *Nat. Rev. Mol. Cell Biol.* **2002**, *3*, 401.
9. (a) Donovan, M.; Olofsson, B.; Gustafson, A. L.; Dencker, L.; Eriksson, U. *J. Steroid Biochem. Mol. Biol.* **1995**, *53*, 459; (b) Fogh, K.; Voorhees, J. J.; Aström, A. *Arch. Biochem. Biophys.* **1993**, *300*, 751; (c) Schug, T. T.; Berry, D. C.; Toshkov, I. A.; Cheng, L.; Nikitin, A. Y.; Noy, N. *Proc. Natl. Acad. Sci. U.S.A.* **2008**, *105*, 7546; (d) Schug, T. T.; Berry, D. C.; Shaw, N. S.; Travis, S. N.; Noy, N. *Cell* **2007**, *129*, 723; (e) Budhu, A. S.; Noy, N. *Mol. Cell. Biol.* **2002**, *22*, 2632.
10. (a) Dekker, F. J.; de Mol, N. J.; van Ameijde, J.; Fischer, M. J. E.; Ruijtenbeek, R.; Redegeld, F. A. M.; Liskamp, R. M. J. *ChemBioChem* **2002**, *3*, 238; (b) Lebeau, L.; Oudet, P.; Mioskowski, C. *Helv. Chim. Acta* **1991**, *74*, 1697.
11. Kita, Y.; Maeda, H.; Takahashi, F.; Fukui, S.; Ogawa, T.; Hatayama, K. *Chem. Pharm. Bull.* **1994**, *42*, 147.
12. Bernardes, G. J.; Grayson, E. J.; Thompson, S.; Chalker, J. M.; Errey, J. C.; El Oualid, F.; Claridge, T. D.; Davis, B. G. *Angew. Chem., Int. Ed.* **2008**, *47*, 2244.
13. (a) Yang, Q. H.; Du, C. *J. Biol. Chem.* **2004**, *279*, 16963; (b) Yang, Y.; Fang, S.; Jensen, J. P.; Weissman, A. M.; Ashwell, J. D. *Science* **2000**, *288*, 874.
14. Compound **7** was designed by removal of the amino group and hydroxyl group from BE04 (**5**). Structure–activity relationship study of MeBS analogs suggested that these two substituents play an important role in cIAP1-degradation activity and binding to cIAP1 (Ref. 6 and Sato, S.; Tetsuhashi, M.; Skine, K.; Miyachi, H.; Naito, M.; Hashimoto, Y.; Aoyama, H. *Bioorg. Med. Chem.* **2008**, *16*, 4685.).
15. (a) Deveraux, Q. L.; Takahashi, R.; Salvesen, G. S.; Reed, J. C. *Nature* **1997**, *388*, 300; (b) Kasof, G. M.; Gomes, B. C. *J. Biol. Chem.* **2001**, *276*, 3238; (c) Vucic, D.; Stennicke, H. R.; Pisabarro, M. T.; Salvesen, G. S.; Dixit, V. M. *Curr. Biol.* **2000**, *10*, 1359; (d) Hao, Y.; Sekine, K.; Kawabata, A.; Nakamura, H.; Ishioka, T.; Ohata, H.; Katayama, R.; Hashimoto, C.; Zhang, X.; Noda, T.; Tsuruo, T.; Naito, M. *Nat. Cell Biol.* **2004**, *6*, 849; (e) Srinivasula, S. M.; Hegde, R.; Saleh, A.; Datta, P.; Shiozaki, E.; Chai, J.; Lee, R. A.; Robbins, P. D.; Fernandes-Alnemri, T.; Shi, Y.; Alnemri, E. S. *Nature* **2001**, *410*, 112; (f) Suzuki, Y.; Nakabayashi, Y.; Takahashi, R. *Proc. Natl. Acad. Sci. U.S.A.* **2001**, *98*, 8662.
16. (a) Gupta, A.; Williams, B. R.; Hanash, S. M.; Rawwas, J. *Cancer Res.* **2006**, *66*, 8100; (b) Gupta, A.; Kessler, P.; Rawwas, J.; Williams, B. R. *Exp. Cell Res.* **2008**, *314*, 3663.
17. (a) Slack, A. D.; Chen, Z.; Ludwig, A. D.; Hicks, J.; Shohet, J. M. *Cancer Res.* **2007**, *67*, 2448; (b) Slack, A.; Chen, Z.; Tonelli, R.; Pule, M.; Hunt, L.; Pession, A.; Shohet, J. M. *Proc. Natl. Acad. Sci. U.S.A.* **2005**, *102*, 731; (c) Chen, L.; Iraci, N.; Gherardi, S.; Gamble, L. D.; Wood, K. M.; Perini, G.; Lunec, J.; Tweddle, D. A. *Cancer Res.* **2010**, *70*, 1377; (d) Kang, J. H.; Rychahou, P. G.; Ishola, T. A.; Qiao, J.; Evers, B. M.; Chung, D. H. *Biochem. Biophys. Res. Commun.* **2006**, *351*, 192.
18. Nara, K.; Kusafuka, T.; Yoneda, A.; Oue, T.; Sangkhathat, S.; Fukuzawa, M. *Int. J. Oncol.* **2007**, *30*, 1189.

FULL PAPER *Bacteriology*

Evaluation of a PCR-Restriction Fragment Length Polymorphism (PCR-RFLP) Assay for Molecular Epidemiological Study of Shiga Toxin-Producing *Escherichia coli*

Norihiko SUGIMOTO[1,3], Kensuke SHIMA[1]**, Atsushi HINENOYA[1], Masahiro ASAKURA[1,3], Akio MATSUHISA[1,3], Haruo WATANABE[2] and Shinji YAMASAKI[1]*

[1]*Graduate School of Life and Environmental Sciences, Osaka Prefecture University, 1–58 Rinku Ourai-kita, Izumisano, Osaka 598–8531,* [2]*Department of Bacteriology, National Institute of Infectious Diseases, 1–23–1 Toyama, Shinju-ku, Tokyo 162–8640 and* [3]*Research and Development Center, Fuso Pharmaceutical Industries, Ltd., 2–3–30 Morinomiya, Jouto-ku, Osaka 536–8523, Japan*

(Received 11 January 2011/Accepted 28 January 2011/Published online in J-STAGE 10 February 2011)

ABSTRACT. In this study, we have evaluated our recently developed polymerase chain reaction-restriction fragment length polymorphism (PCR-RFLP) assay for the molecular subtyping of Shiga toxin-producing *Escherichia coli* (STEC). A total of 200 STEC strains including O157 (n=100), O26 (n=50), O111 (n=10), and non-O26/O111/O157 (n=40) serogroups isolated during 2005–2006 in Japan, which were identified to be clonally different by pulsed-field gel electrophoresis (PFGE) were further analyzed by the PCR-RFLP assay in comparison to PFGE. Ninety-five of O157, 48 of O26, five of O111 and 19 of non-O26/O111/O157 STEC strains yielded one to three amplicons ranging from 6.0 to 15.5 kb in size by the specific primer set targeting region V which is located in the upstream of *stx* genes. These strains were classified into 41 (O157), 8 (O26), 4 (O111) and 17 (non-O26/O111/O157) groups based on the RFLP patterns obtained by subsequent restriction digestion, respectively. Although the discriminatory power of PCR-RFLP assay was somewhat less than that of PFGE, it is more convenient for molecular subtyping of STEC strains especially for O157, the most important serogroup implicated in human diseases, as well as to identify the outbreak-associated isolates because of its simplicity, rapidity, ease and good reproducibility.

KEY WORDS: *E. coli*, molecular epidemiology, molecular typing, PCR-RFLP, STEC.

J. Vet. Med. Sci. 73(7): 859–867, 2011

Shiga toxin-producing *Escherichia coli* (STEC) has emerged as an important food-borne pathogen infecting thousands of people every year in Japan, and US [22]. Shiga toxin (Stx), the prime virulence factor of STEC, is classified into two groups namely Stx1 and Stx2 on the basis of their immunological properties [38]. Both Stx1 and Stx2 are encoded on lambda-like bacteriophage, so-called Stx-phage [38, 39]. Although more than 400 serotypes of STEC strains have been reported, O157:H7 is the most important serotype associated with human diseases such as hemorrhagic colitis and hemolytic-uremic syndrome [32, 38, 39] and is also the most predominant serotype isolated from sporadic cases and outbreaks [11, 45]. Since most of the food-poisonings caused by STEC are related to the consumption of beef or beef products, cattle have been considered as a major source of infection [5]. Other vehicles such as contaminated water, vegetables, and fruits have also been considered to be infection source of STEC [1, 4, 33]. Furthermore, person-to-person transmission is also an important factor for STEC infection [13, 31].

Several molecular subtyping methods such as ribotyping, randomly amplified polymorphic DNA-PCR, pulsed-field gel electrophoresis (PFGE), multi-locus sequence typing (MLST), multiple-locus variable-number of tandem repeats analysis (MLVA) etc. have been developed and utilized for molecular epidemiological studies of STEC [6, 10, 21, 28, 29, 44]. Among these, PFGE is the most commonly used molecular typing method to identify the possible source and route of infection, and has been used for a variety of pathogens including STEC because of its high discriminatory power to reveal their clonal relationships [3, 40]. However, PFGE has some disadvantages [13, 15, 23, 35]. For instance, PFGE requires expensive and elaborate equipment, and skilled labor. PFGE is labor-intensive and fairly time-consuming. PFGE profiles of some strains cannot be analyzed because of smeared profiles, which may be associated with degradation of genomic DNA due to free radical produced during electrophoresis [8, 18, 37]. PFGE pattern of a single isolate of STEC could be altered by repeated subcultures *in vitro* [13, 36]. Passage through bovine or human gastrointestinal tract could also cause variation in PFGE patterns for STEC strains [2, 15]. Thus, there is a chance of misinterpretation of clonality of the same strain. In addition, it is not possible to handle large number of samples at a time [16].

Sato *et al.* identified 6 characteristic regions (I to VI) in Shiga toxin phage genome [33]. Among them, region V, which is located in the upstream region of the Stx2 operons, was identified to be the most distinct portion in the entire phage genome and may be a good target for molecular sub-

* CORRESPONDENCE TO: YAMASAKI, S., Graduate School of Life and Environmental Sciences, Osaka Prefecture University, 1–58 Rinku Ourai-Kita, Izumisano, Osaka 598–8531, Japan.
e-mail : shinji@vet.osakafu-u.ac.jp

** PRESENT ADDRESS: SHIMA, K., Institute of Medical Microbiology and Hygiene, University of Lübeck, Ratzeburger Allee 160, 23538 Lübeck, Germany.

typing of STEC strains. For this reason, we have developed a rapid and simple DNA fingerprinting method, PCR-restriction fragment length polymorphism (PCR-RFLP) assay based on the nucleotide sequence diversity within the region V of Stx-phage, for molecular epidemiological study of STEC strains [34–37]. In the present study, we have evaluated the PCR-RFLP assay targeting the region V of Stx-phages by using a variety of defined STEC strains including O157 and non-O157, which were identified to be clonally different by PFGE.

MATERIALS AND METHODS

Bacterial strains and growth media: A total of 200 STEC strains of various serogroups, including O157 (n=100), O26 (n=50), O111 (n=10) and non-O26/O111/O157 (n=40) were randomly selected from 1,795 strains which were provided from the prefectural and municipal health centers and public health institutes (PHIs) in Japan during 2005 to 2006. Serology was determined and all strains were identified to be different clone by PFGE at the National Institute of Infectious Diseases under the National Epidemiological Surveillance of Infectious Diseases undertaken in compliance with the Law Concerning the Prevention of Infectious Diseases and Medical Care for Patients of Infections [25, 26]. STEC strains used in this study were cultured either on L-agar or in L-broth.

Chemicals and enzymes: Chemicals were purchased either from Nacalai Tesque (Kyoto, Japan), Wako Pure Chemical Industries (Tokyo, Japan), or Sigma Chemical Co. (St. Louis, MO, U.S.A.). Restriction enzymes, Takara LA Taq, and LA PCR kit version 2 were purchased from Takara Bio (Shiga, Japan). Bacto tryptone and yeast extract were purchased from Becton, Dickinson and Company (Franklin Lakes, NJ, U.S.A.). Pulsed-field certified, low-melting point preparative-grade, Seakem GTG and Seakem HGT (for high gelling temperature) agaroses, were either from Bio-Rad Laboratories, Inc. (Hercules, CA, U.S.A.) or Takara Bio. Molecular weight makers were purchased from Takara Bio.

Detection of stx1 and stx2 genes by multiplex PCR: Presence of *stx1* and *stx2* genes was examined by multiplex PCR using EVT-1 and EVT-2 primers, and EVS-1 and EVC-2 primers, respectively, as described in Table 1 [30]. Briefly, 50 μl of overnight culture of STEC strains was added to 450 μl of TE buffer and the mixture was boiled for 10 min and snap cooled on ice. After centrifugation at 10,000 g for 10 min, supernatant was collected and stored at –30°C for further use as boiled template. PCR was carried out in 20 μl of reaction mixture for each tube containing 1 μl of DNA template, 1 × PCR buffer (10 mM Tris-HCl [pH 8.3], 50 mM KCl, and 1.5 mM $MgCl_2$), 0.2 mM of dNTP, 0.625 U of rTaq polymerase (Takara Bio Inc.) by using GeneAmp PCR system 2400 (Perkin-Elmer, Wellesley, MA, U.S.A.). PCR primer and conditions are described in Table 1. The PCR products were subjected to 2.0% agarose gel electrophoresis in TAE (40 mM Tris-acetate [pH 8.0], 1 mM EDTA) buffer followed by staining in ethidium bromide solution (2 $\mu g/ml$) and destaining in distilled water for 5–10 min each. Images were captured by Gel-Doc 2000 (Bio-Rad Laboratories).

PCR-RFLP: PCR was performed in a GeneAmp PCR System 2400 (Perkin-Elmer) using primer sets targeted to the region V or upstream region of *stx* genes in Stx-phage as shown in Fig. 1 and Table 1. The PCR products were analyzed by 0.4% agarose gel electrophoresis using HGT agarose and/or by field inversion gel electrophoresis using 1.0% pulsed-field certified agarose gel in 0.5 × TBE (45 mM Tris-borate [pH 8.0], 1.0 mM EDTA) buffer for 16 hr followed by staining with ethidium bromide (2 $\mu g/ml$). In these electrophoreses, a 1-kb or 2.5-kb DNA ladder (Takara Bio. Inc.) was used as the molecular mass standard. The run condition was generated by the autoalgorithm mode of CHEF Mapper pulsed-field gel electrophoresis (PFGE) system with a size range of 6 to 15 kb. The PCR products were further restric-

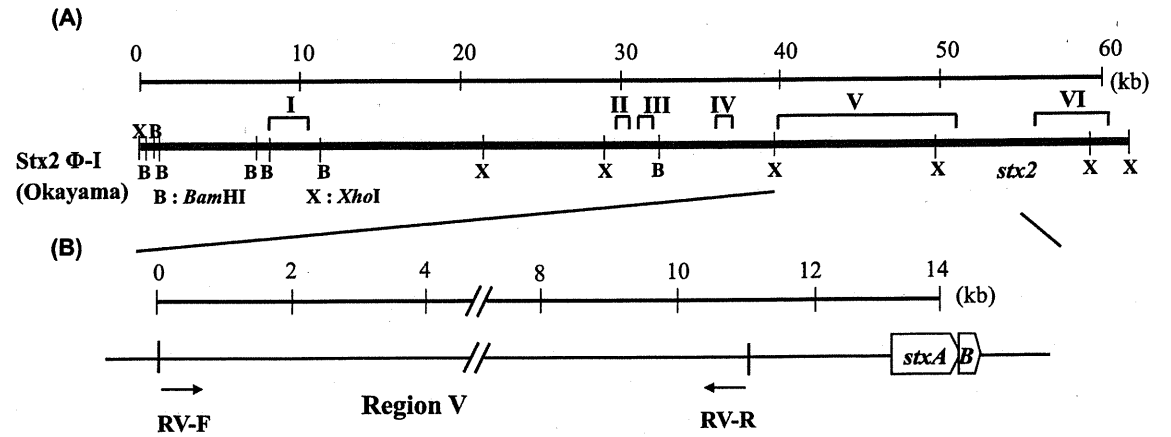

Fig. 1. (A) Restriction map of the Stx2ϕ-I genome and the location of six characteristic regions (I to VI). B and X represent *Bam*HI and *Xho*I, respectively. (B) Enlargement of the region V where PCR primer binding sites are located. Arrow indicates the location of primers, such as RV-F, and RV-R, respectively (Table 1).

Table 1. PCR primer and conditions used in this study

Primer	Sequence (5'–3')	Target	Aim	First denaturing	PCR conditions			Cycles	Amplicon	Reference
					Denaturing	Annealing	Extension			
EVT-1	CAACACTGGATGATCTCAG	*stx1*	Multiplex PCR	94°C 5 min	94°C 30 sec	55°C 30 sec	72°C 1 min	35	349 bp	[30]
EVT-2	CCCCCTCAACTGCTAATA									
EVS-1	ATCAGTCGTCACTCACTGGT	*stx2*		94°C 5 min	94°C 30 sec	55°C 30 sec	72°C 1 min	35	110 bp	[30]
EVC-2	CTGCTGTCACAGTGACAAA									
RV-F	GACATTGCTCCGTGTATTCACTCGTTGGAA	Region V	PCR-RFLP	94°C 1 min	98°C 20 sec	68°C 10 min[a)]		30	Variable	[37]
RV-R	ATTTTGCATTTCCTTCGCGCTGGTTTAGCC									

a) Annealing and extension steps were performed at the same time.

tion digested for 2 hr either by 10 U of *Bgl*I or 8 U of *Eco*RV. The digested products were then analyzed by 1.5% agarose gel electrophoresis and/or by field inversion gel electrophoresis using 1.0% pulsed-field certified agarose gel in 0.5 × TBE buffer for 18 hr. A 1-kb DNA ladder and a 2.5-kb DNA ladder (Takara Bio. Inc.) were used as molecular mass standards. The run condition was generated by the autoalgorithm mode of CHEF Mapper PFGE system with a size range of 1 to 10 kb for the *Bgl*I digest or 1 to 6 kb for the *Eco*RV digest. A model 1000 Mini-Chiller (Bio-Rad Laboratories) was used to maintain the temperature of the buffer at 14°C. The gels were stained and destained by similar way as mentioned above. The photographs of the electrophoretic patterns of the digested DNA (PCR-RFLP) were captured and recorded digitally using gel documentation system (Gel-Doc 2000, Bio-Rad Laboratories).

Data analysis: The discriminatory power of the PCR-RFLP typing for different O serogroup was evaluated using the Simpson's index of diversity as described previously [12].

RESULTS

Detection of stx1 and stx2 genes by multiplex PCR: A total of 200 STEC strains including 100 of O157, 50 of O26, 10 of O111 and 40 of other serogroups were analyzed for the presence of *stx1* and *stx2* genes by the multiplex PCR [30]. In O157 serogroup, 5, 46 and 49 strains were found to be positive for *stx1*, *stx2* and both *stx1* and *stx2* genes whereas in O26 serogroup 48 and 2 strains were positive for *stx1* and both *stx1* and *stx2* genes, respectively. In case of O111, 6 were positive for *stx1* and 4 for both *stx1* and *stx2* genes, while in case of non-O26/O111/O157, 20, 14 and 6 were positive for *stx1*, *stx2* and both *stx1* and *stx2* genes, respectively (Table 2).

PCR-RFLP for Shiga toxin-producing E. coli: Boiled templates of 200 STEC strains including 100 of O157, 50 of O26, 10 of O111 and 40 of non-O26/O111/O157 were amplified by primer set RV-F and RV-R and one to three amplicons ranging from 6.0 to 15.5 kb in size were yielded from 95 of O157, 48 of O26, 5 of O111 and 19 of non-O26/O111/O157 strains (Figs. 2A and 3A, Table 2). Subsequently PCR products obtained from 167 STEC strains were digested with either *Eco*RV or *Bgl*I and the RFLP patterns were compared to each other among each category of serogroups. Figs. 2B and 3B show the representative RFLP patterns of *Eco*RV digest whose discrimination ability is higher than those of *Bgl*I digest. In the case of O157, *Eco*RV digest yielded 4 to 11 fragments ranging from 450 bp to 5.7 kb in size (Fig. 2B) and *Bgl*I digest yielded 2 to 9 fragments ranging from 500 bp to 9.6 kb in size (data not shown). Although RFLP patterns of O157–30 (lane 31) and O157–31 (lane 32) by *Eco*RV were identical, those were differentiated by *Bgl*I digest (data not shown). In the case of O26, *Eco*RV digest yielded 4 to 14 fragments ranging from 150 bp to 4.4 kb in size (Fig. 3B, Lanes 2–9) while in O111, 5 to 6 fragments ranging from 900 bp to 8.5 kb were obtained by *Eco*RV digest (Fig. 3B, Lanes 10–13). In the case of non-O26/O111/O157, 2 to 12 fragments ranging from 150 bp to 5.7 kb were obtained by *Eco*RV digest (Fig. 3B, Lanes 14–30). Based on the RFLP profiles, 95 O157, 48 O26, 5 O111 and 19 non-O26/O111/O157 strains were classified into 41, 8, 4 and 17 groups, respectively (Tables 2 and 3).

DISCUSSIONS

Molecular typing methods have played important roles to trace the route of infection and identify the strain associated with outbreak, in particular diffuse outbreak [40]. Among them, PFGE is currently the most widely used molecular subtyping method for detecting outbreaks of *E. coli* O157:H7 because of its high resolution and reproducibility. However, there are several disadvantages and limitations in PFGE as described above. Therefore, the use of PCR-based method such as PCR-RFLP may be an alternative because of several benefits. For example, the PCR-RFLP (1) does not require special equipment, although FIGE was used in this study, a simple mini gel electrophoresis unit such as MUPID (Advance Co., Ltd., Tokyo) can be applicable, (2) can analyze large number of strains at the same time, (3) can complete rapidly within a day, (4) can analyze the RFLP without isolation of the strain [34], (5) can avoid smearing due to free radical produced during electrophoresis [37], and (6) is not affected by repeated subculture of a single isolate *in vitro* and passage through bovine or human gastrointestinal tract [35, 36]. In addition, (7) it is not necessary to send STEC strains but genomic DNA is enough in order to compare the RFLP patterns at two different laboratories, which is safer and easier to ship. For this reason, we have developed a simple, rapid and easy molecular subtyping method such as PCR-RFLP assay on the basis of genetic diversity of region V in Stx-phage and have shown its various utilities